We approve the thesis of Daniel Trevitz.

Date of Signature

Dr. Sean Brennan
Associate Professor of Mechanical Engineering
Thesis Advisor

Dr. Mark Horn
Professor of Engineering Science and Mechanics
Academic Adviser

Judith A. Todd
Professor, Department of Engineering Science and Mechanics
P. B. Breneman Department Head

991734320

THE PENNSYLVANIA STATE UNIVERSITY

DEPARTMENT OF ENGINEERING SCIENCE AND MECHANICS

MECHANICAL DESIGN, MODELING, AND CONTROL OF A THREE DEGREE-OF-FREEDOM PARALLEL MECHANISM IMPLEMENTED ON A QUADRUPED ROBOT

Daniel Trevitz
Spring 2013

A thesis
submitted in partial fulfillment
of the requirements
for a baccalaureate degree
in Engineering Science
with honors in Engineering Science

Reviewed and approved* by the following:

Dr. Sean Brennan
Associate Professor of Mechanical Engineering
Thesis Advisor

Dr. Mark Horn
Professor of Engineering Science and Mechanics
Academic Adviser

Judith A. Todd
Professor, Department of Engineering Science and Mechanics
P. B. Breneman Department Head

*Signatures are on file in Engineering Science and Mechanics Office.

Abstract

In this thesis the viability of a rigid three degree of freedom parallel mechanism, utilized as a robotic leg, was evaluated. The parallel aspect of the mechanism gives the system a relatively low inertia, making the mechanism mechanically responsive and easy to control. The mechanism was evaluated using a series of prototypes to develop the mechanism as a leg. After development of a leg the system was implemented as a quadrupedal robot for analysis. The robot was evaluated for maneuverability, rigidity, and durability. The mechanism performed adequately as a leg during the tests. The mechanism and robot were rigid enough to allow repetitions of a given motion without noticeable drift. During testing, the system showed the ability to perform tasks such as stair climbing, sitting, and kicking a ball.

Table of Contents

Chapter 1

Introduction

This thesis demonstrates the design, construction, usage, control, and focus on the further development of a three degree-of-freedom parallel mechanism developed, by Dr. Adelstein, The mechanism implemented as the legs on a quadrupedal robot for analysis. The primary objective of the capstone project is to determine if the three degree-of-freedom mechanism can be used as the legs of a robotic walker. Other objectives focus on improving the performance, cost, time to manufacture, and demonstrate the capability of the mechanism as a leg. The capstone project was funded by Dr. Sommer, Dr. Brennan, and the writer of this thesis.

The development of the mechanism into a leg is motivated by the potential uses for legged robotics. Wheeled vehicles have several advantages over legged vehicles including better mechanical efficiency and better stability at high speeds. However, wheeled vehicles can not access more than half of the Earth land mass [1]. For example, wheeled vehicles traditionally have a difficult time traversing rough or chaotic terrain.

The leg considered in this study is a parallel manipulator instead of the typical serial manipulator. A serial manipulator is one which achieves multiple degrees of freedom by chaining linkages and joints together. In contrast, the leg considered here is a parallel mechanism where the actuators for the 3 degree-of-freedom are always located on one plane. The most significant advantage of this approach is that the end effector is substantially lighter. The low inertia allows the mechanism to rapidly reposition without overshoot, making the task of controlling the mechanism simpler.

1.1 Literature Review

The 3 degree-of-freedom mechanism of interest in this thesis was designed by Dr. Bernard Adelstein of NASA. Patented October 6th 1998, the mechanism was designed for use as a measurement tool [2]. An individual would grasp the ball, labeled D, at which point movement by the individual along the directions a, b, or c would be measured by rotary motion sensors located at A, B, and C as seen in Figure-1.1.

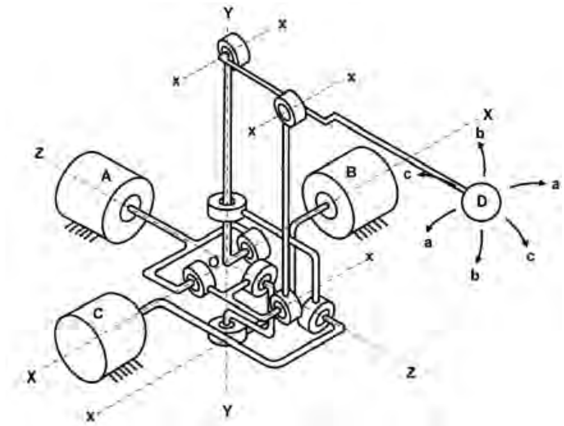

Figure 1.1: Edited version of Figure 1 from US Patent 5,816,105 [2]

In Figure-1.1 there are nine revolute joints in the mechanism and three revolute joints at A, B, and C. All of the joints are capable of movement only about a single axis. This makes the mechanism very ridged allowing for precise positioning compared to other 3 degree-of-freedom mechanisms [3].

The mechanism is capable of placing the end effector, labeled D, anywhere within a subset of three space. The motion is primarily restricted to revolve about point O ad locking B, giving a spherical range of motion with constant radius. By including the rotation of B the mechanism gains the ability to move freely.

The system created by Mr. Miller who built a single instance implementation of the patented mechanism for his MS thesis at UIUC[3]. His resulting design, shown in Figure-1.2, is a demonstration of a fully developed version of the mechanism. The system was created to demonstrate the controllability and precision of the mechanism. This was done by attaching a free inverted pendulum to the end effector of the mechanism. The inverted pendulum was attached using two revolute joints and position sensors on each joint. Miller's resulting system was able to balance a 3D inverted pendulum atop the mechanism [3].

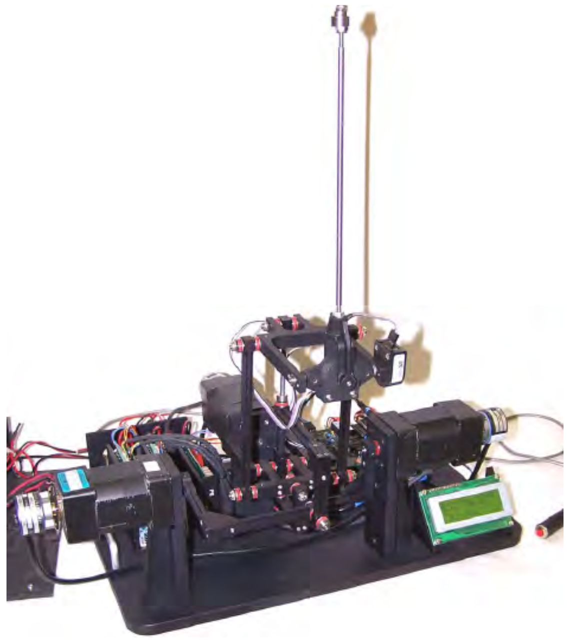

Figure 1.2: Figure A.2 from Page 56 of Miller's Thesis [3]

The position sensors mounted to the pendulum allowed for the system to position itself such that the pendulum would always be erect. The dynamics of the open-loop system are unstable but demonstrated that the system was capable of stabilizing the pendulum [3]. The previous work on the mechanism by Miller demonstrates that the mechanism is accurate, controllable, difficult to model, and requires a large amount of precision for assembly. Additionally the mechanism as designed by Miller is expensive to build and requires a large amount of time to fabricate the linkages.

Chapter 2

3 Degree of Freedom Mechanism

2.1 Mechanism Operation

Understanding the motion of the ridged links that comprise the mechanism is a nontrivial task due to the parallel nature of the mechanism. In the most extreme case, movement along two axis simultaneously in the global reference frame can cause every link to move simultaneously relative to one another. Therefore to properly understand and evaluate the mechanism, the principle of superposition is applied. While superposition does not apply fully to this nonlinear mechanism, it does apply around a local operating point because the kinematic equations are sufficiently smooth to allow local linearization of motion around an operating point via Taylor expansions. Shown in Figure-2.1 is the mechanism divided into the three primary motion paths. The assumption is made that the motion along a, b, or c can be analyzed individually and then recombined after analysis. The result is assumed to be similar, if not identical, to a simultaneous analysis.

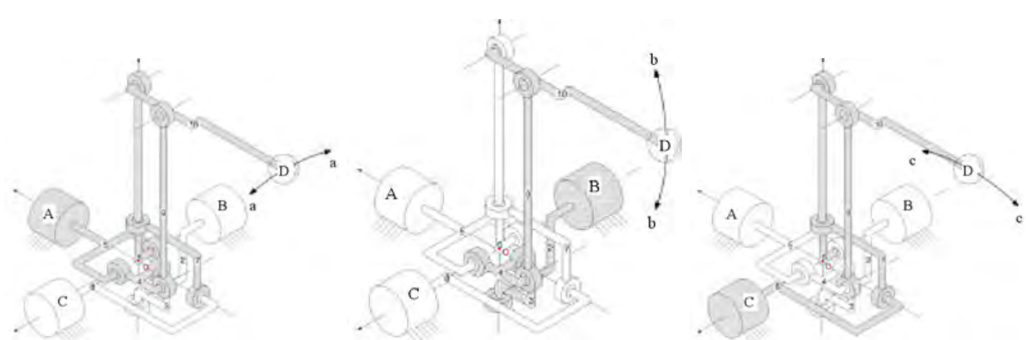

(a) A motion component (b) B motion component (c) C motion component

Figure 2.1: Motion of the mechanism for a single component [4]

Every joint, shown in the diagram as a wheel and hub, is only capable of revolute motion along a single axis. The grounded cylinders, representing actuators or sensors, are capable of rotation only about either the x or z axis. In each of the figures in Figure-2.1, the grayed linkages are the linkages which rotate when the end effector moves along the indicated path. When multiple paths are traversed simultaneously, the linkages will translate and rotate. Because of the mobility of the rotational joints, the simultaneous equations can become involved. A point of interest is given any motion of the end effector, labeled D, link 6 will rotate about point O. Point O will only rotate about Point O as a result of the mechanism's design.

2.2 Adaptations

Adelstein's design was extended by Miller for use as an actuator rather than a motion sensor [3, 4]. As seen in Figure-1.2 the most visible change is the addition of symmetry about the z axis of the mechanism. When in the position shown in Figure-1.2 and Figure-2.1, the internal torques of the system are more balanced. This balance allows for the applications of greater loads to the end effector. The additions also reduce the range of vertical motion; however, the reductions force the ranges of motion to be symmetrical.

The design used here is based on Mr. Miller's drawings and adapted to be built from plastic rather then metal [3]. This allowed for rapid prototyping and made machining the parts significantly easier. The use of bearings in the mechanism was avoided for the purpose of alleviating the cost and complexity to build the mechanism.

The majority of the reinforcing parts were removed to ease the design process. As testing continues on the mechanism, reinforcement beyond the anticipated requirements of the parts can be added as needed. The removal of support parts was facilitated by the combinations of several parts within a single link.

For a robotic walker, the motion along path-b, shown in Figure-2.1b, is of importance when climbing stairs. Without the addition of a joint that can act as a knee, the mechanism must have sufficient range of motion to push the end effector over the ledge of the step. The end effector, connected to link 10 in Figure-2.1, is the final link in a four bar mechanism. The length of link 10 changes the mechanical efficiency of the motion along path b and the range of motion. The length of link 10 can be chosen relative to link 4 based on the weight of the robotic walker. A shorter length will have more lifting force in the leg, but less range of motion and slower walking speeds of the robot.

2.3 Nomenclature

The nomenclature that will be used for the remainder of this thesis differs from the nomenclatures used by Adelstein and Miller. The nomenclature was designed to allow for complete definition of the mechanism linkages as well as be clear enough to be used for kinematic analysis.

Each link was renamed with a letter name and given a coordinate frame using the same letter. The origin of coordinate frame was left free for all the analysis done in this thesis. Given a generic coordinate frame, q, the axes of the coordinate frame are labeled q_1, q_2, and q_3 as seen in Figure-2.2. The nine coordinate frames a through i are part of the mechanism, the X coordinate frame is attached to the frame, and the $X-Y-Z$ frame is the global reference frame. Seen in Figure-2.2 is an isometric view of an example leg shown in the standard anatomical position. In this position the direction of the first coordinate points out of the page, the second coordinate points into the page, and the third points to the top of the page.

$$\phi_{ab} = \hat{a}_2 \angle \hat{b}_2 \tag{2.1a}$$
$$\phi_{cd} = \hat{c}_2 \angle \hat{d}_2 \tag{2.1b}$$
$$\phi_{bf} = \hat{b}_2 \angle \hat{f}_2 \tag{2.1c}$$
$$\phi_{di} = \hat{d}_2 \angle \hat{i}_2 \tag{2.1d}$$

$$\theta_1 = \hat{x}_2 \angle \hat{e}_2 \tag{2.2a}$$
$$\theta_2 = \hat{x}_1 \angle \hat{c}_1 \tag{2.2b}$$
$$\theta_3 = \hat{x}_3 \angle \hat{a}_3 \tag{2.2c}$$

$$\gamma = \hat{e}_3 \angle \hat{i}_3 = \hat{e}_3 \angle \hat{h}_3 \tag{2.3a}$$
$$\beta = \hat{e}_3 \angle \hat{i}_3 = \hat{e}_3 \angle \hat{h}_3 \tag{2.3b}$$
$$\alpha = \hat{e}_1 \angle \hat{f}_1 = \hat{e}_1 \angle \hat{g}_1 \tag{2.3c}$$

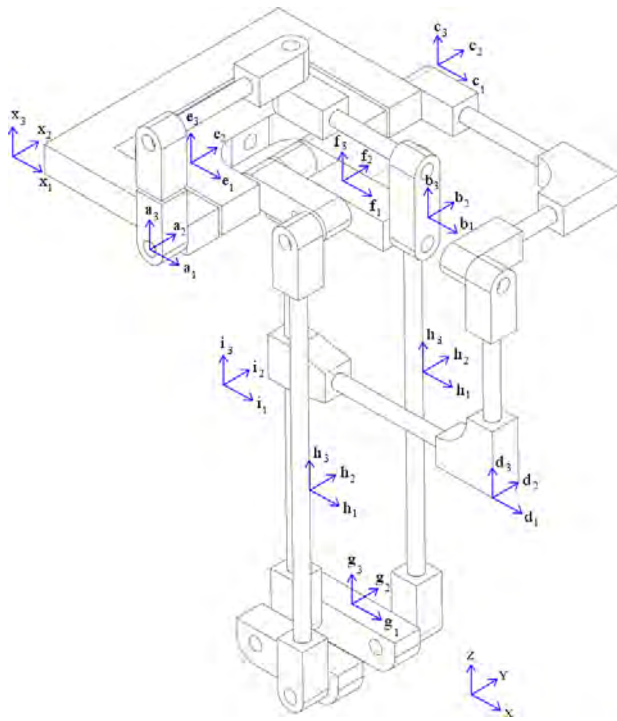

Figure 2.2: Isometric view of an example leg in the standard anatomical position

Equation-(2.1),(2.2), & (2.3) are the definitions for the internal angles.

2.4 Part Relations

A set of equations were developed to mathematically define the linkages. These equations define the physical sizes of each part in relation to other parts. The result is the parts can easily be joined in the mechanism and the ranges of motion easily predicted. Each link was defined with the intention of reusing the definitions in the analysis of the mechanism.

The linkages are defined using the letter for the name and the axis number as a subscript. For example, link-a has two lengths of importance along the second and third axis. The length of link-a along the second and third axes are called a_2 and a_3 respectively. The resulting simplified vector of link-a is $r_a = \{0, a_2, a_3\}$. Each linkage dimension is primarily defined in terms of other linkages, with a few defined to avoid linkage collisions, and the remaining defined to set the overall size of the mechanism.

The assumption was made that maximum diameter, d_b, of all holes within a part would be no more than one half the thickness of the material. This was implemented by defining the thickness of the material to be twice the diameter of the holes. The available material was 0.25"thick thus $d_b = 0.125$". The mechanism was developed here without bearings; however, if bearings where to be included, the outer bearing diameter would be d_b. For this project d_b was defined as the thickness of the bolts used for all the joints.

Chapter 3

Prototypes

Six prototypes were built for this project. Presented in this chapter are the first four prototypes developed. Chapter-5 presents the fifth prototype, which was the first to be motorized. The sixth prototype, the first quadrupedal prototype and final outcome of this project, is discussed in Chapter-6.

3.1 Lego 1

The first prototype was developed with the goal of better understanding Millers drawings [3]. The motion of the mechanism was the primary objective to learn from this. By analyzing the motion of the linkages the alignments of the joints and the function of the joints were observed. The alignment requirements were included in later designs, as discussed in Chapter-5.

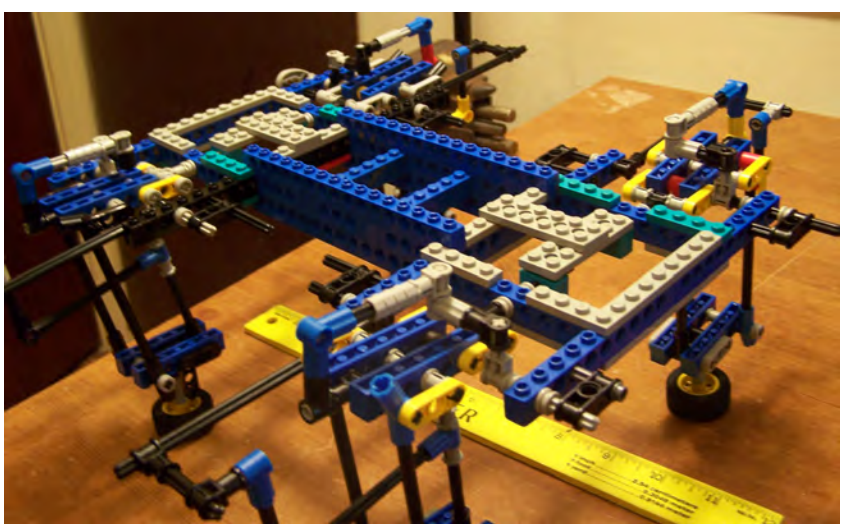

Figure 3.1: First Lego based prototype

Other aspects studied were the placement and functionality of the feet, the motion of the third axis, locations of high stress, and the impact of the joints on the precision of the mechanism's movement.

3.2 Lego 2

The second prototype was developed to test the mechanism when under a torque. The gear train for each motor has a 25:1 gear down ratio. The motors are estimated to have a stall torque of 3.3Ncm at 5V [5]. During tests, the system never stalled and was more than capable of lifting itself off of the ground. The motor torque multiplied by the gear ratio divided by two legs per motor gives 59 oz-in. of torque required on the servo motor to be able to self-lift the mechanism. This demonstrates that a standard hobby servo, which easily exceeds this torque requirement, will be able to manipulate the mechanism when used as a leg.

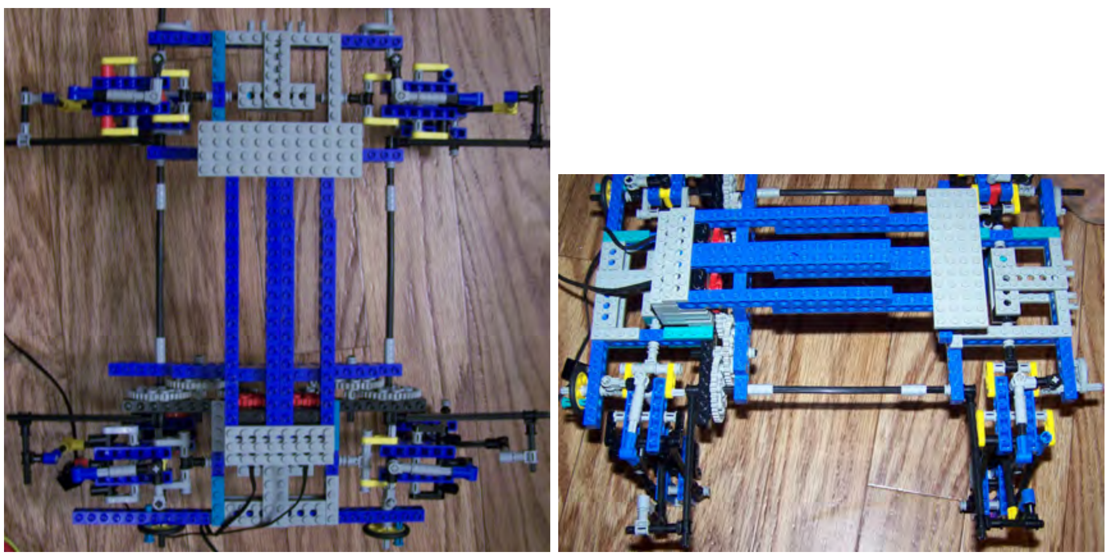

Figure 3.2: Second Lego based prototype

3.3 Laser 1

The development of this prototype was the first to involve manufacturing all parts. The parts were developed in SolidWorks and exported to a dxf file for cutting with an Epilog Helix 24, 60 Watt, CO_2 laser cutter. The parts where then drilled with a drill press, and tapped with a hand tap. The threaded rod was cut to length with a hack saw and the burrs removed with a file. The assembly was straight forward and required one improvisation: one of the threaded rods had to have a slot cut so it could be turned by a driver.

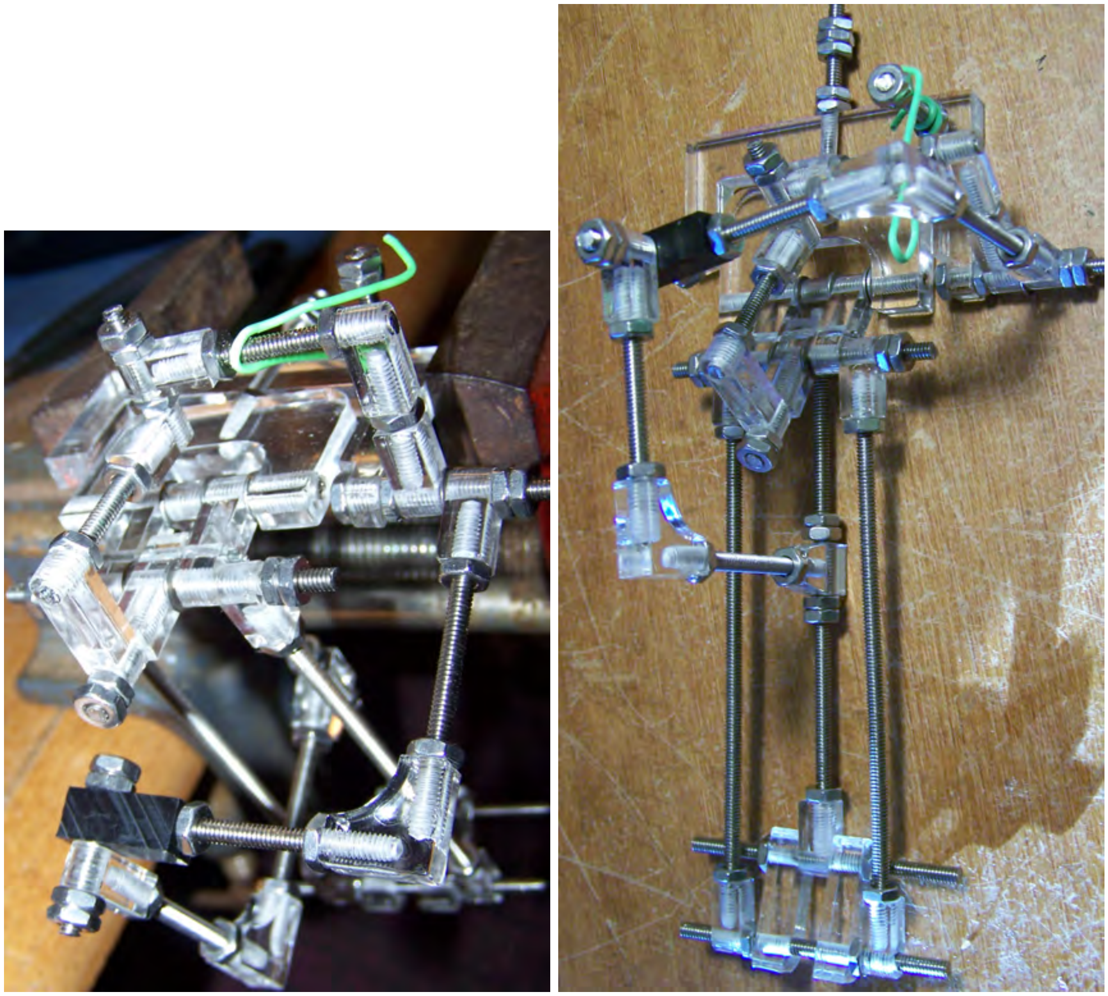

Figure 3.3: First Laser cut Prototype

While the design was functional a few parts were broken during the machining. Additionally all of the parts were smaller than anticipated as a result of the thickness of the laser beam. The final disadvantage of the design was the amount of time for complete assembly. This design required 8 hours of machining and assembly which was felt to be excessive. Thus, subsequent designs made efforts to simplify both the mechanism and the assembly process.

3.4 Laser 2

The fourth prototype was designed with the intention of reducing the part count in the center of the mechanism. The result was a significantly shorter assembly time, with decreased capacity for alignment of the joints. The change required more precision during manufacturing of the pieces but gave the linkages greater rigidity. Additionally by removing the metal rod the price and weight of the mechanism was decreased.

Figure 3.4: Second Laser cut Prototype

Chapter 4

Mechanism Kinematics

The kinematics of the mechanism have several uses which extend outside the scopr of this thesis. They are developed here for the purpose of creating an accurate model of the mechanism for the selection of servos for the system. The equations can also be used in future work for the control of the mechanism

4.1 Method

To analyze the kinematics of the mechanism, each unique link was given a coordinate frame. The coordinate frames were then related using the rotation matrices given in Equations-(4.1).

The mechanism consists of single degree of freedom revolute joints, therefore the following rotation matrices were used to relate the coordinate frames from each link. Given a vector from one coordinate frame that vector can be translated to a rotated frame using the rotation matrices by matrix premultiplication.

$$R_1(\alpha) = \begin{pmatrix} 1 & 0 & 0 \\ 0 & \cos(\alpha) & -\sin(\alpha) \\ 0 & \sin(\alpha) & \cos(\alpha) \end{pmatrix} \tag{4.1a}$$

$$R_2(\alpha) = \begin{pmatrix} \cos(\alpha) & 0 & \sin(\alpha) \\ 0 & 1 & 0 \\ -\sin(\alpha) & 0 & \cos(\alpha) \end{pmatrix} \tag{4.1b}$$

$$R_3(\alpha) = \begin{pmatrix} \cos(\alpha) & -\sin(\alpha) & 0 \\ \sin(\alpha) & \cos(\alpha) & 0 \\ 0 & 0 & 1 \end{pmatrix} \tag{4.1c}$$

Each coordinate frame was defined while the mechanism was in the standard anatomical position for a quadruped, as seen in Figure-4.1.

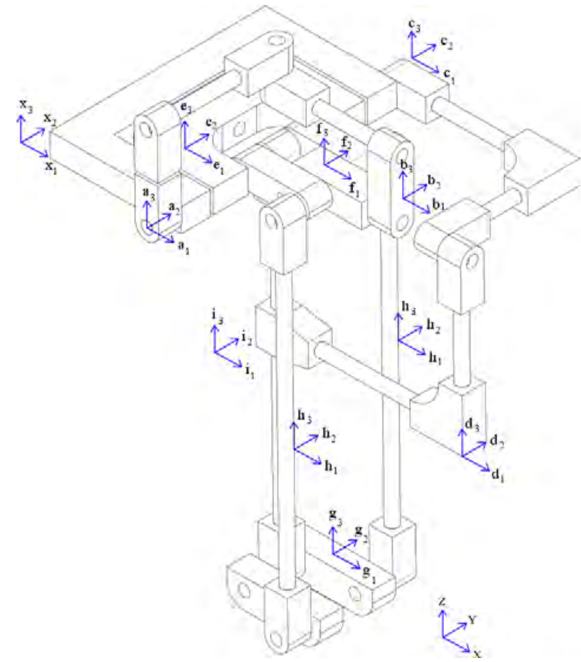

Figure 4.1: Definition of the 11 unique reference frames

Each coordinate frame was given a letter name that is the same as the part name. The exception to this is the frame of the mechanism which was given the X coordinate frame. In the standard anatomical position the first axis of each coordinate frame is aligned with the global X-axis, the second with the global Y-axis, and the third with the global Z-axis.

After the coordinate frames were defined each part was defined in terms of vectors. The vectors use the link length definitions from the nomenclature defined in Section-2.3. The vectors are defined by the length of the parts as r_q or defined between two joints as r_{qw}. Equation-(4.2) gives the part vectors used in this chapter.

$$r_a = \{0, -a_2, a_3\} \tag{4.2a}$$
$$r_b = \{b_1, 0, -b_3\} \tag{4.2b}$$
$$r_c = \{c_1, c_2, 0\} \tag{4.2c}$$
$$r_d = \{-d_1, 0, -d_3\} \tag{4.2d}$$
$$r_e = \{e_1, 0, 0\} \tag{4.2e}$$
$$r_{fh} = \{f_1, 0, 0\} \tag{4.2f}$$
$$r_{fb} = \{f_{p1}, 0, 0\} \tag{4.2g}$$
$$r_h = \{0, 0, -h\} \tag{4.2h}$$
$$r_g = \{g_1, 0, 0\} \tag{4.2i}$$
$$r_{gh} = \{g_1 - f_1, 0, 0\} \tag{4.2j}$$
$$r_{id} = \{0, 0, -i_a\} \tag{4.2k}$$
$$r_{dg} = \{0, 0, -i_b\} \tag{4.2l}$$
$$r_{x1} = \{0, 0, 0\} \tag{4.2m}$$
$$r_{x2} = \{x_1, x_2, 0\} \tag{4.2n}$$
$$r_{x3} = \{x_1, x_2, 0\} \tag{4.2o}$$

Several simplification can be applied to reduce the complexity of the equations that use Equation-(4.2). The main simplifications are given in Equation-(4.3)

$$x_1 = e_1 \tag{4.3a}$$
$$a_2 = c_2 = x_2 \tag{4.3b}$$
$$a_3 = b_3 \tag{4.3c}$$
$$c_1 = d_1 \tag{4.3d}$$
$$f_{p1} = b_1 \tag{4.3e}$$
$$d_3 = i_a \tag{4.3f}$$

4.2 Forward Kinematics

The forward kinematics can be defined in terms of the internal angles γ, β, and α. The forward kinematics are found by taking the sum of the part vectors r_h, $r_f h$, and $r_g h$ from Equation-(4.2) converted to the e reference frame and then rotated to the X reference frame.

$$R_1(\gamma)\left(R_2(\beta)r_h + R_2(\alpha)r_{fh} + R_2(\alpha)r_{gh}\right) = \begin{pmatrix} -h\sin(\beta) + g_1\cos(\alpha) \\ \sin(\gamma)\left(h\cos(\beta) + g_1\sin(\alpha)\right) \\ -\cos(\gamma)\left(h\cos(\beta) + g_1\sin(\alpha)\right) \end{pmatrix} \tag{4.4}$$

The internal angles γ, β, and α can be defined in terms of θ_1, θ_2, and θ_3 to complete the kinematic equations. By definition the angle between e_3 and X_3 is given by θ_1 and γ for uniformity. α and β can be found by creating two closed loop vector equations made from four multi-linkage vectors.

$$\text{links\_}ab = r_{x3} + R_2(\theta_3)\left(r_a + R_3(\phi_{ab})r_b\right) \tag{4.5a}$$
$$\text{links\_}cd = r_{x2} + R_2(\theta_2)\left(r_c + R_1(\phi_{cd})r_d\right) \tag{4.5b}$$
$$\text{links\_}ef = r_{x1} + R_1(\theta_1)\left(r_e + R_2(\alpha)r_{fb}\right) \tag{4.5c}$$
$$\text{links\_}ed = r_{x1} + R_1(\theta_1)\left(r_e + R_2(\beta)r_{id}\right) \tag{4.5d}$$

The two loop equations of interest give two vector equations.

$$0 = \text{links\_}ab - \text{links\_}ef$$
$$0 = \begin{pmatrix} -\cos(\alpha) + \cos(\theta_3)\cos(\phi_{ab}) \\ -\sin(\alpha)\sin(\theta_1) + \sin(\phi_{ab}) \\ \cos(\theta_1)\sin(\alpha) - \cos(\phi_{ab})\sin(\theta_3) \end{pmatrix}$$
$$0 = \text{links\_}cd - \text{links\_}ed$$
$$0 = \begin{pmatrix} \sin(\beta) - \cos(\phi_{cd})\sin(\theta_2) \\ -\cos(\beta)\sin(\theta_1) + \sin(\phi_{cd}) \\ \cos(\beta)\cos(\theta_1) - \cos(\theta_2)\cos(\phi_{cd}) \end{pmatrix}$$

The vector equations can then be used to create two equations by relating ϕ_{ab} and ϕ_{cd} terms.

$$\cos(\phi_{ab}) = \frac{\cos(\alpha)}{\cos(\theta_3)} = \frac{\cos(\theta_1)\sin(\alpha)}{\sin(\theta_3)} \tag{4.6}$$
$$\cos(\phi_{cd}) = \frac{\sin(\beta)}{\sin(\theta_2)} = \frac{\cos(\beta)\cos(\theta_1)}{\cos(\theta_2)} \tag{4.7}$$

From Equation-(4.6) and Equation-(4.7) the solutions to alpha and beta are given in Equation-

(4.8) and Equation-(4.9).

$$\tan(\beta) = \cos(\theta_1)\tan(\theta_2) \tag{4.8}$$

$$\tan(\alpha) = \sec(\theta_1)\tan(\theta_3) \tag{4.9}$$

4.3 Actuator Kinematics

The mechanism is powered by three rotary actuators. Each actuator is connected to the end effector through a series of linkages. Using the same method as was used for the forward kinematics, a set of equations were developed that could be used in a static analysis. To solve for the static torque requirements of each actuator, the relation between the end effector and the actuators can be used. Noting that each actuator is primarily controlling one range of motion, the static analysis is divided into three segments, one for each actuator.

When the mechanism is put into the standard anatomical position, one actuator is free to move at a time, and assuming that only one motion is powered by one servo, the static analysis is straight forward. Using Equations-(4.8) and Equations-(4.9), the values for α and β can be found for each actuator.

For actuator one $\theta_2 = \theta_3 = 0$, setting $\alpha = \beta = 0$. This sets the d, e, f, g, h, and i reference frames to be identical. For actuator two $\theta_1 = \theta_2 = 0$, setting $\alpha = 0$ and $\beta = \theta_2$, which sets the c, d, h, and i reference frames to be identical. Note that the angle between the i and g reference frames are $-\beta$. For actuator three $\theta_1 = \theta_2 = 0$, we see that $\alpha = \theta_3$, $\beta = 0$, and $\phi_{ab} = \phi_{bf} = 0$. Equations-(4.10a),(4.10b), & (4.10c)

$$L_1 = R_1(\theta_1)\,(r_e + r_{dg} + r_g + r_{id}) \tag{4.10a}$$

$$L_2 = R_2(\theta_2)\,(r_c + r_{dg} + r_d + R_2(-\beta)r_g) \tag{4.10b}$$

$$L_3 = r_a + r_b \tag{4.10c}$$

Using the simplifications given in Equation-(4.3), Equation-(4.10) can be reduced to the Equation-(4.11).

$$L_1 = \{e_1 + g_1, h\sin(\theta_1), -h\cos(\theta_1)\} \tag{4.11a}$$

$$L_2 = \{-h\sin(\theta_2) + g_1, x_2, -h\cos(\theta_2)\} \tag{4.11b}$$

$$L_3 = \{b_1, -a_2, 0\} \tag{4.11c}$$

Chapter 5

Mechanism Construction

The purpose of this thesis project is to design and analyze the performance of the mechanism when implemented as a leg. In this chapter the process for prototyping, the method for the selection of the servos, and the instructions for construction are given.

5.1 Leg Design Notes

For prototyping University Park's Learning Factory provides an Epilog laser cutter which can be used to cut up to 0.25" thick acrylic. The laser cutter accepts a drawing file which can be created directly from SolidWorks, the solid modeling software used for this project. To increase the number of prototypes made the laser cutter was used and the acrylic plastic was selected based on the plastic available at Dr. Brennan's lab.

By using 0.25" acrylic, any bearings used in the mechanism require the axles to be too thin to support loads. As a result bearings were not used in design and 0.125" diameter fully threaded rod was used as the axle for all the joints and as fasteners within the mechanism. Typically, a design for a joint would not include threaded rod on plastic for reasons of friction and durability. Because the design is a prototype, longevity was not considered in the design. The friction of the threaded rod on the acrylic was found in the earlier prototypes to be negligible. The rod was purchased in 3' lengths and then cut to length.

5.2 Servo Selection

To select a servo that can be used in both a single leg and for quadrupedal robot the dimensions of the leg had to be built in scale with available servo technologies. The second Lego prototype, shown in Section-3.2, required approximately 59oz-in of torque from each servo for a relatively difficult task. After viewing several standard servos this torque was deemed reasonable the dimensions of the Lego prototype was carried over to the final design.

In Equation-(4.11) the value of h, the effective height of the leg, is the primary factor for the required strengths of servos one and two. The greater the value for h, the greater the mobility of the leg, and the more torque needed from the servos. A typical quadrupedal gait requires three legs to support the robot. Estimating that the weight of the robot is evenly distributed, the load each leg must support is one third the total weight.

Servos one and two control the dominant degrees of freedom, side to side and front to back, of the leg. The analysis of each servo involves determining the force applied along the servo arm to hold a static load. The forces along each arm are defined by rotating the force vector, due to gravity, from the ground frame into the g frame. The force vector is composed to the weight of the robot, W, along the vertical, X_3, axis.

$$f_{g\alpha} = R_1(\theta_3).\{0, 0, W\} \tag{5.1a}$$

$$f_{g\beta} = R_2(0).\{0, 0, W\} \tag{5.1b}$$

$$f_{g\gamma} = R_1(-\theta_1).\{0, 0, W\} \tag{5.1c}$$

By assuming the mechanism is fixed, the first and second degrees of freedom are simple levers. The third degree of freedom, responsible for raising and lowering the foot, is a four bar mechanism which gives a mechanical advantage that must be included. For the third degree of freedom, by relating the torques of parts f and g, the following ratio is found.

$$f_f = \frac{f_{p1}}{g_1} f_{g\alpha} \tag{5.2}$$

Using the force equations and the servo arm lengths from Equation-(4.11), the torques required by each servo are given as Equation-(5.3).

$$\tau_1 = L_1 \times f_{g\gamma} = W\left\{h\sin(2\theta_1), -\cos(\theta_1)\left(e_1 + g_1\right), \sin(\theta_1)\left(e_1 + g_1\right)\right\} \tag{5.3a}$$

$$\tau_2 = L_2 \times f_{g\beta} = W\left\{x_2, h\sin(\theta_2) - g_1, 0\right\} \tag{5.3b}$$

$$\tau_3 = L_3 \times f_f = -W\frac{f_{p1}}{g_1}\left\{\cos(\theta_3)a_2, \cos(\theta_3)b_1, \sin(\theta_3)b_1\right\} \tag{5.3c}$$

Equation-(5.3) includes all of the torques expected on the shaft of the servo when there is no support included in the design. Of most interest for the servo selection are the torques along the shaft of the servo. For servo 1, the torque is along X_1 and for servos two and three the torque is along X_2. Note that the orientation of servo 3 is opposite that of servo 2 requiring a negation of the servo angle when calibrating the servo.

Using the results of Equation-(5.3), the stall torques for each servo can be found. In order to simplify the control of the servos, the choice was made to use the same servo for servos one, two, and three. Thus, only the peak loads of normal operation by all the servos were considered. Extracting the components of interest from Equation-(5.3) gives the following:

$$\tau_1 = W * h \sin(2\theta_1) \tag{5.4a}$$

$$\tau_2 = W * (h \sin(\theta_2) - g_1) \tag{5.4b}$$

$$\tau_3 = -W * b_1 \frac{f_{p1}}{g_1} \cos(\theta_3) \tag{5.4c}$$

The weight of the robot, W, was estimated as the weight of the twelve servos, the frame, a 10oz. battery, 5oz of electronics, and a 16oz. payload. The frame is assumed to be one third the weight of the 12 servos. Evaluating Equation-(5.4a) at $\theta_1 = \pi/4$, the max torque is $\tau = \text{Weight} * h$. Given this result, the servo selection was narrowed to support a leg height, h, of 3"to 5". The EXI D226F servo was chosen setting the servo weight to 2.1oz. and the stall torque at 180 oz-in.

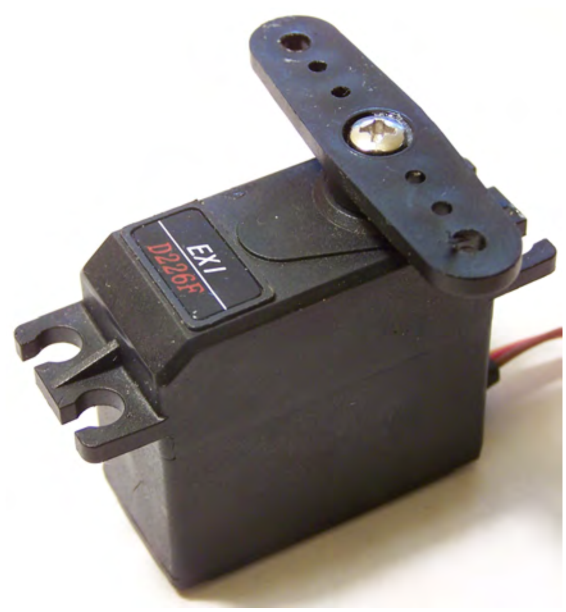

Figure 5.1: EXI D226F Servo

After initial selection of the servo, a value of 5"was chosen for h, and the total weight was set at 66oz., giving 22oz. for the three legs. Using the maximum of Equation-(5.4a) the max torque desired is 22oz * 5in = 110oz-in, which is within the stall torque of the EXI D226F servo.

5.3 Leg Assembly Notes

The construction of one leg involves cutting, machining, and assembly. Each part is first designed in SolidWorks, assembled into a dxf file, a sheet of acrylic is cut into the parts, each part is machined, the threaded rod is cut to length, and the parts are assembled. The process of machining the parts is lengthy and requires several hours of relatively high precision for hand machining.

While machining the parts, care must be taken when drilling the parts to maintain alignment of the pieces. In particular, parts e and f must be well aligned with the frame of the leg. Most of the frame pieces are adjustable by design, but parts e and f are not. Shown in Figure-5.2a is an example of how to check the alignment after completion of assembly. The rods demonstrate that the parts are aligned along the critical dimensions. This technique can be extended further in order to demonstrate that parts a, b, c, and d are in alignment with the frame.

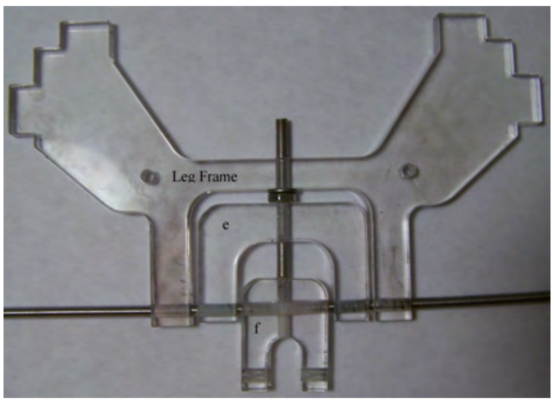

(a) Parts e, f, and the frame in alignment

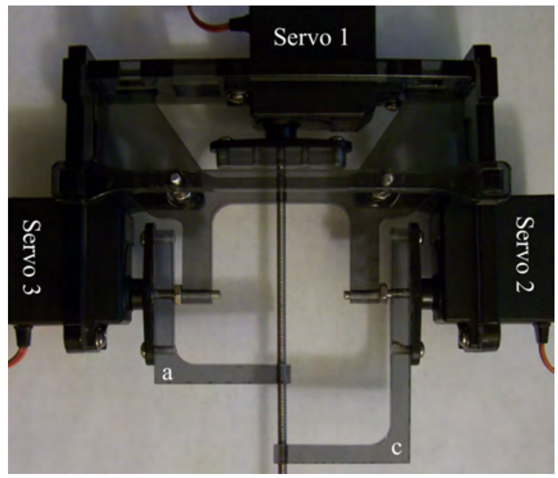

Figure 5.2: Demonstration of the alignment of critical pieces

When tapping the acrylic, if the tap begins to feel tight, make sure to immediately back the tap out and remove the shavings. After taping, it is important to run the threaded rod through the threads a few times to finish the threads. Preparing the threads with the threaded rod prevents parts from loosening during use.

5.4 Leg Assembly Process

The assembly of the machined parts can be completed in several steps. The following is a recommended procedure for the assembly of a single leg.

1. Assemble parts e, f, and i_a with a single threaded rod. The threaded rod, after being cut to length, can have a slot cut into one or both ends to allow for a driver to turn the rod.

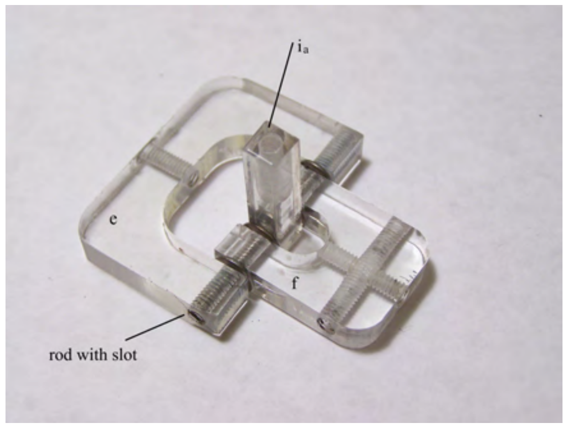

Figure 5.3: Mechanism core assembly

2. Assemble the two feet, part g, part i_b, and two part h.

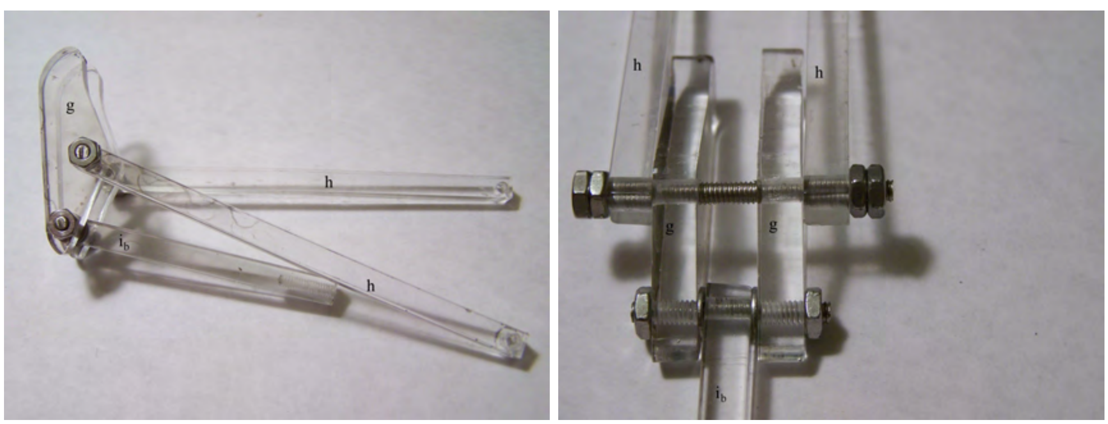

Figure 5.4: Foot Assembly

3. Attach a servo to the servo 1 frame. Attach a horn adapter to the servo. Connect the horn adapter to part e through the leg frame.

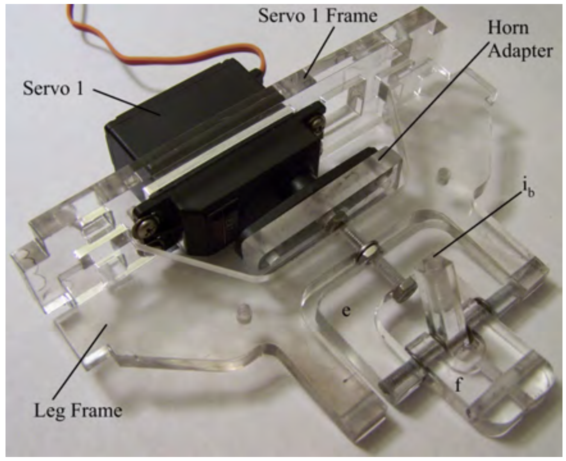

Figure 5.5: Servo one connected to the core assembly

4. Assemble parts d. i_a, and i_b. Take care to not have any extra space between parts i and d as the clearance will decrease the rigidity of the leg significantly. Additionally the end to end height of i_a to i_b should be as close to the height of h as possible.

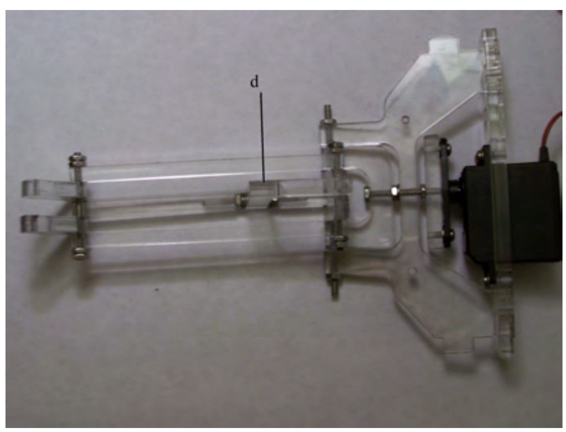

Figure 5.6: Foot and leg frame assemblies

5. Zero the servos by sending them the command to move to the position you want to be the midpoint in their motion and then connect the servo horns to the servos. Make certain to align the third servo's horn perpendicular to the leg frame and the second servo horn parallel to the leg frame as shown in Figure-5.7.

6. Attach servos 2 and 3 to the servo 2 and 3 frame. Attach part a to the servo three horn and part c to the servo two horn. If needed add washers between part a or c and the servo horn to prevent bending the parts from uneven servo horns.

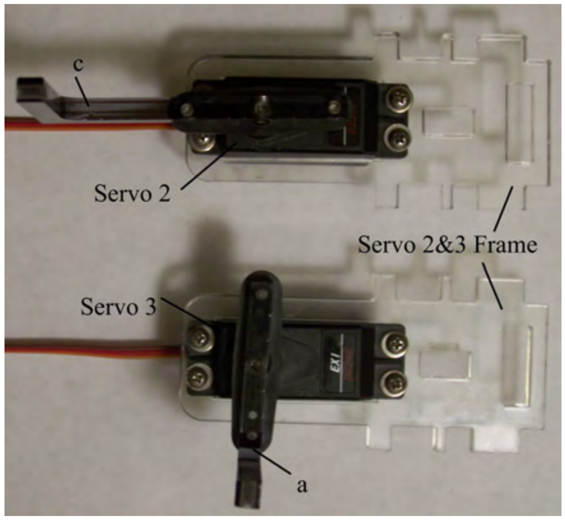

Figure 5.7: Servo two and three assemblies

7. Attach the servo assemblies from the previous step to the leg frame.

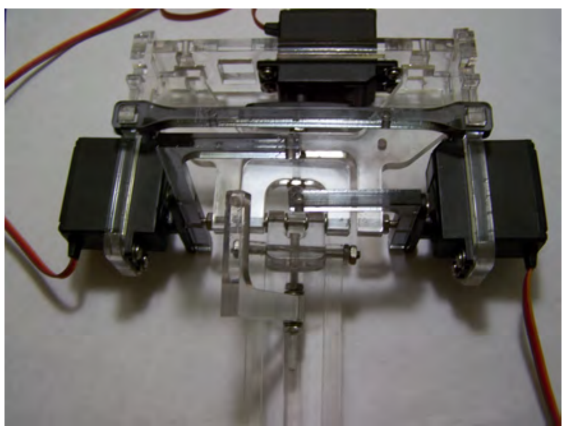

Figure 5.8: Servos and frame assembled

8. Finish the assembly by attaching part b to f, a to b, and c to d.

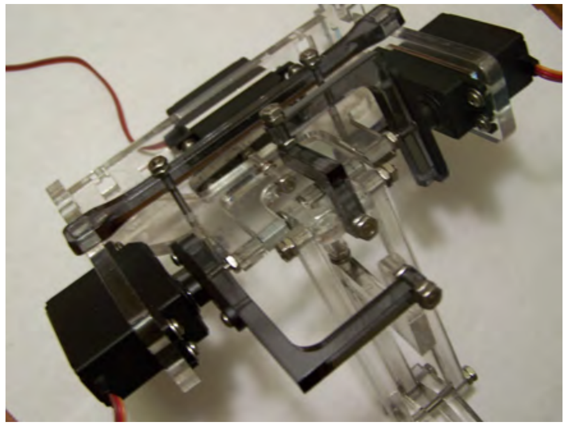

Figure 5.9: Assembled leg

For the single leg model, a sled was added to the back of the leg. Tests were conducted to determine the mobility of the mechanism, showed the design was rigid, had sufficient range of motion, and there was no unexpected collisions.

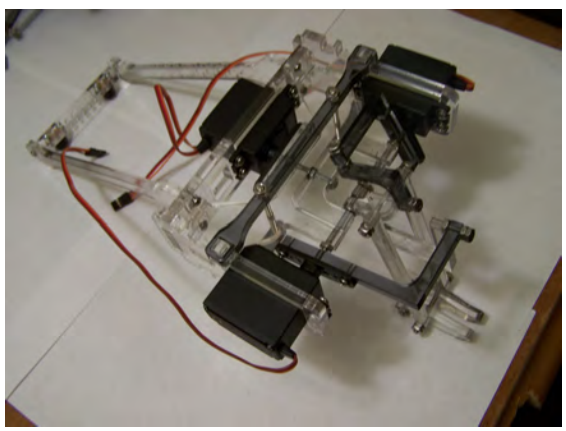

Figure 5.10: Completed single leg ‘dragger’ prototype

The maximum range of θ_1 was 130°, θ_2 was 270°, and θ_3 was 240°. When rotating θ_2 or θ_3 the other would need rotated to avoid collision before the maximum range was reached. Several expected collisions were found to be manageable. Parts b and d frequently collided when the difference of the angle of θ_2 and θ_3 was less than 30°, as show in Figure-5.11a. Additional collisions occurred between the frame and part h when the leg was rotated and elevated. When rotating, the collision could be avoided by lowering the foot.

The possibility of the mechanism inverting the four bar, which means causing the foot to turn upside down, was avoided by connecting the sets of Part h to Part g with a single threaded rod. The rod forced a collision between Part i_b and the rod when the toes were pointed upward and θ_2 was rotated to cause the foot to move towards Servo 1. Under the same conditions, it is also possible for collision between Part h and Part e to occur before the collision of the rod and Part

i_b can occur. The collisions of i and the rod is shown in Figure-5.11b.

Collisions between Part b and Part d, shown in Figure-5.11a occurs at the same point regardless the angles of servo 2 and 3. Noting that the end of Part b sweeps out a circular path, Part d could be redesigned to be circular or extended. The result is that the range of servo 2 and 3 would be increased so the collision of Part $\mathrm{i_a}$ and Part f would occur simultaneously with the collision between Parts b and d. To increase the range of motion after that point, Part f would need to be modified to allow Part $\mathrm{i_a}$ a greater range. Increasing the range of the mechanism is only beneficial if the servos can rotate to their extremes; however, these kind improvements will allow servo 2 and 3 to rotate over more of their respective ranges before collision.

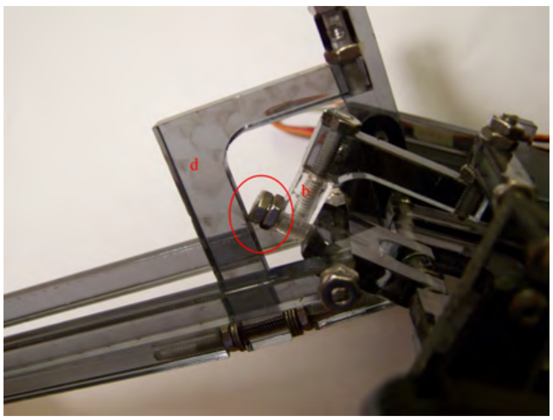

(a) Collision between part d and b

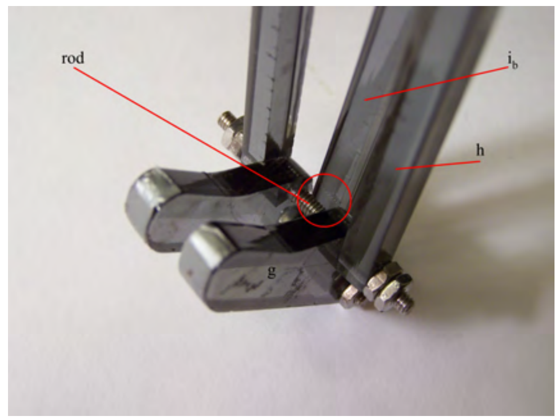

(b) Collision between part i and the rod

Chapter 6

Mechanism Testing and Results

6.1 Robot Assembly

To facilitate the analysis of the mechanism as a leg, a quadrupedal form was chosen for implementation. Four legs were chosen over six primarily for cost purposes, with the option of increasing the leg count if experimentation showed the legs to not be strong or stable enough for mobility.

After the development of a single leg, the design was improved and the quadruped robot was built. Several design alterations where required to improve the stability of the robot. The alterations are documented with the drawings in Appendix-A.

Most of the parts for the leg were designed to have symmetry. This symmetry allows the same series of parts to be assembled in different orientations. The result is a single design that can be assembled such that the four legs are symmetric about the robot's frame. The advantages of using a symmetric design is the weight of the servos are distributed evenly, and the main configurations of the leg can be evaluated simultaneously. The main disadvantage is each leg may act differently increasing the complexity of controlling the robot.

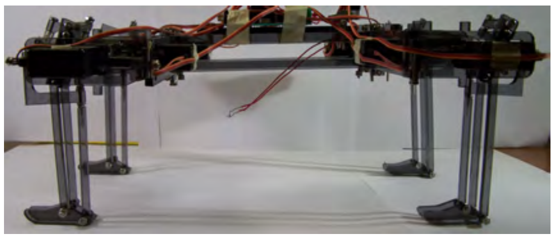

(a) Left View, front is on the left

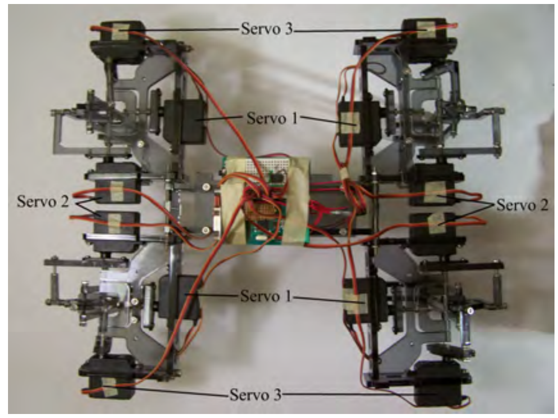

(b) Top View, front is on the left

Figure 6.1: Assembled robot

To facilitate the analysis of the mechanism as a leg, a quadrupedal form was chosen for implementation. Four legs were chosen over six primarily for cost purposes, with the option of increasing the leg count if experimentation showed the legs to not be strong or stable enough for mobility. The orientation of the mechanisms was chosen to better simulate mammalian mobility. The mechanism does not have uniform ranges of motion, as a result the second degree of freedom of the mechanism was oriented front to back.

Shown in Figure-6.1 is the first prototype of the quadruped robot. Figure-6.1 shows the different configurations of the legs in the robot. Servo 2 was placed towards the center because Part c extends the most from the leg. The Servo 1 Frame was positioned such that the majority of Servo 1 faces the center of the robot. Part g is oriented so the toes point in the same direction. The result is the rear servo threes operates in reverse to that of the forward servo threes.

For this thesis the twelve servos were controlled by a Parallax Propeller Demo Board. The Propeller was programed to accept input from a serial port to reposition a servo. The Propeller was given the commands from a desktop program. The program was configured to run scripts containing preset angles and manual control for positioning the servos. Care must be taken when positioning the mechanism because a collision between two parts often results in one of the parts breaking or the frame flexing.

6.2 Robot Testing

Despite difficulty for generating procedures for locomotion, the robot was capable of performing actions such as kicking a ball, some stair climbing, sitting, laying, and standing on two legs. The stair climbing was a moderate success as the robot could climb with the front legs quite adequately. A procedure for climbing with both legs was not developed. Kicking a ball was quite successful but not very effective as the maximum speed of the leg was low. Sitting and laying where simple tasks as well as standing back up from either position.

The primary difficulty during testing came from the inability of the robot to shift weight from one leg to another. Without knees, the robot must remove all weight from one leg before moving the leg forward. The front legs where capable of moving one foot on point and raising the opposing leg, but this was not true for the rear legs. The cause appears to be due to the different foot orientations. Because the rear legs are assembled with the toes pointing towards Servo 1, the weight, when raising the toes, is transfered to Parts i instead of Part h. This slight difference in weight distribution causes the action of going on point with a front leg to raise the other front leg, while putting a rear foot on point causes the same side's front foot to raise.

Shown in Figure-6.2 are several of the basic motions the robot could perform. Basic locomotion was performed by the robot, but the gait was chaotic and non-repetitive. The primary difficulty was that as the robot would move forward the overall height would lower to the point that the legs could not both clear the ground and not bind internally. Several other difficulties were overcome by making the feet have a poor grip on the surface of travel.

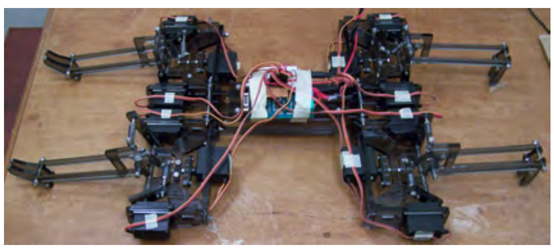

(a) Robot spread eagle

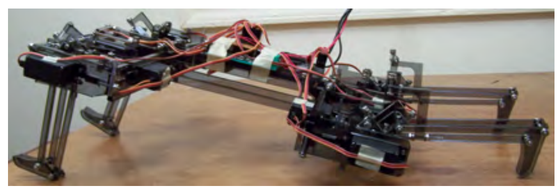

(b) Standing up after laying

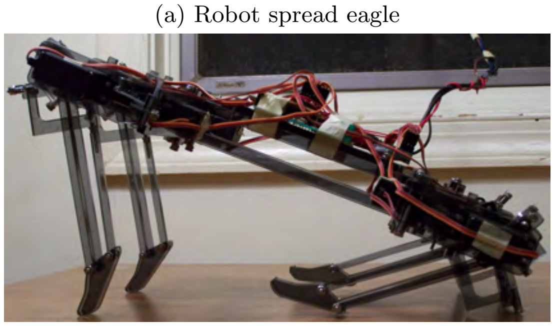

(c) Robot Sitting

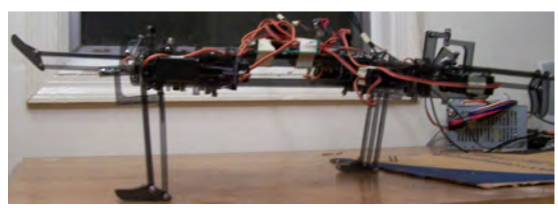

(d) Two Leg Balance

Figure 6.2: Basic Motions

The process for climbing stairs was successful to a point. The robot was capable of moving up several stairs with the front legs. Due to the length of the robot the stairs needed to be longer for both legs to climb. By increasing the number of stairs climbing with all legs could have been tested.

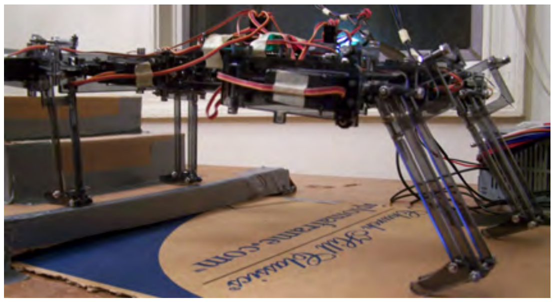

(a)

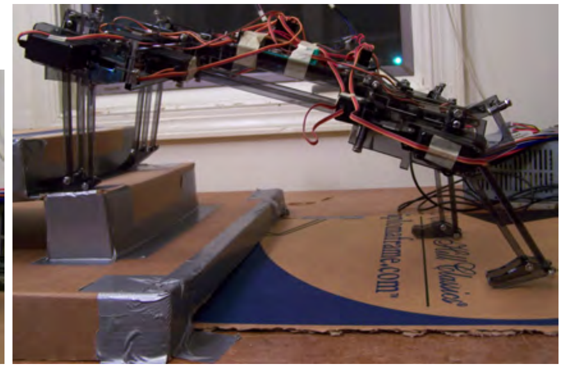

(b)

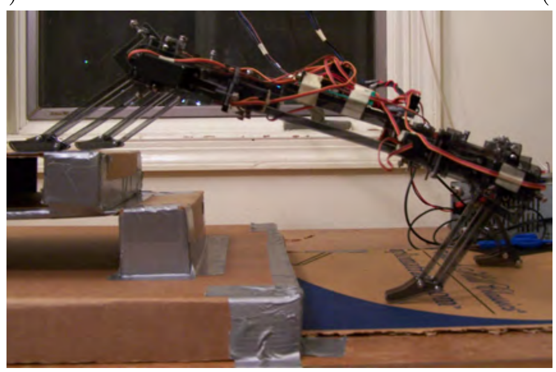

(c)

Figure 6.3: Stair Climbing

6.3 Results & Conclusions

The servos selected performed adequately for position control, could position themselves promptly without overshoot and supplied the torque needed. The stall torque was much greater than the linkages and snapped several parts. While the servos were capable of position control, the maximum speed is not impressive. Given the results of the equations from Chapter-5, the servos could be selected to have a lower torque to achieve a higher speed. The toes are controlled by servo 3. Under normal operating the torque requirements where much lower than the stall torque; however, at large angles the torque did increase to the point of staling the current design.

The current design for attaching Part e to Servo Horn 1 uses a threaded rod and the action of double nutting to fasten the connection. While under moderate loads, Part e often turns loose. The current assembly process does not include any adhesive which could prevent this. Another method would be using a pin through the part and the rod or a set screw.

Rigidity of the robot was low due to movement of the frame pieces. When under high load the Leg Frame would flex, demonstrating a weakness in the design of the part. In addition to the frame flexing, several parts were not perfectly rigid as a result of the joint design. Due to slack between the shaft and the threaded rod the parts could move out of alignment. This primarily affected Part f because the load on the leg is transmitted through the joint internal to Part f.

In conclusion the mechanism developed by Dr. Adelstein and Mr. Miller can be adapted for use as a leg. The performance of the leg was found to be promising but the leg will need more development before more complicated tasks can be performed.

Appendix A

Drawings

The following drawings are of the parts used in the robot. Part g and the Support Plate were not used in the final prototype and are improvements on the last version built. The Servo 2&3 Frame where also updated to connect to the Support Plate. Note that the Spine, Frame End, Servo 1 Frame, and Servo 2&3 Frame do not show the holes for attaching to the Support Plate. As a result of the support plate it is likely that Frame Brace 1 will be not be needed and could be used exclusively on the exterior Servo 2&3 Frames.

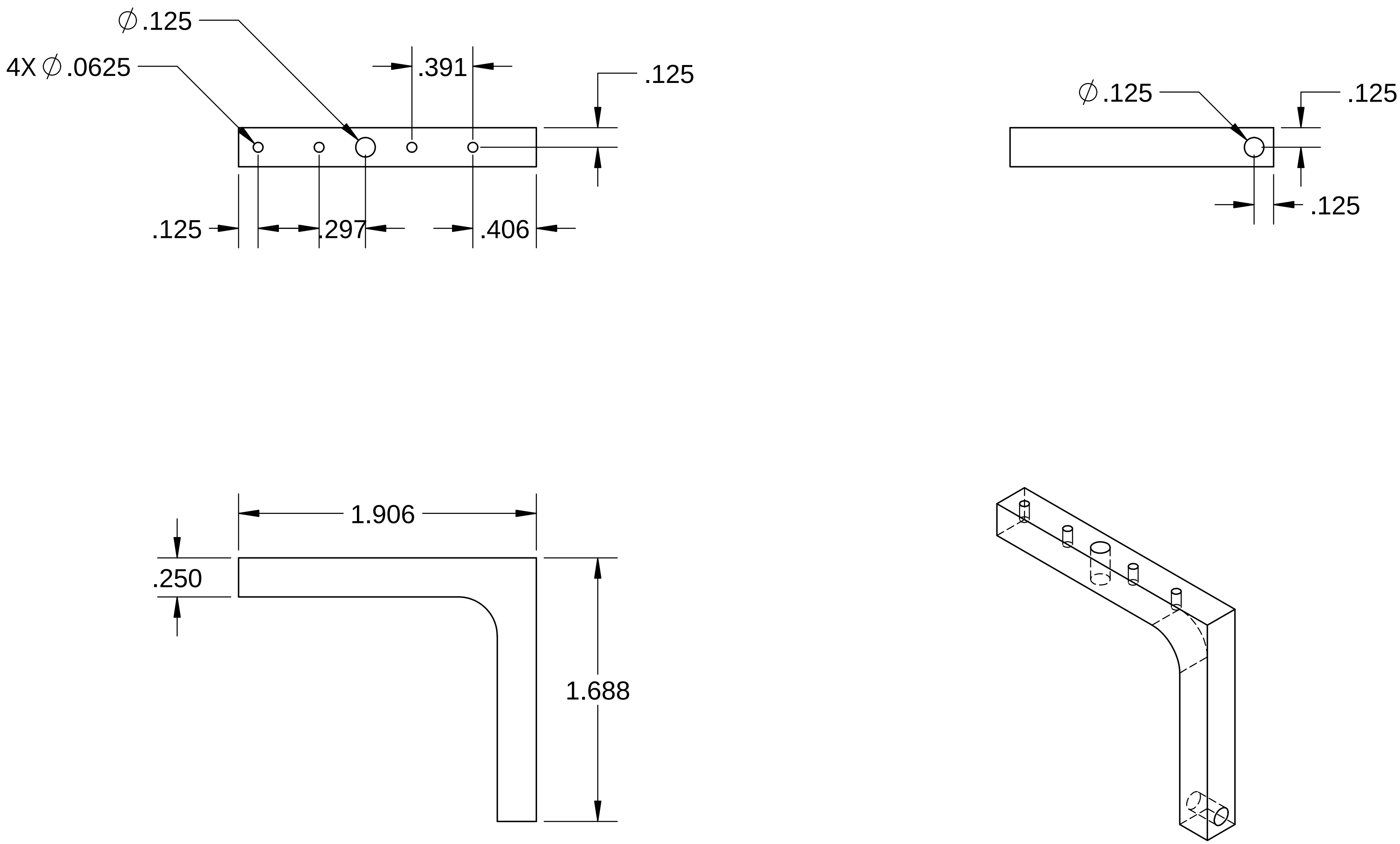

SIZE A

Title

Part a

SCALE: 1:1

DIMENSIONS ARE IN INCHES

5 4 3 2 1

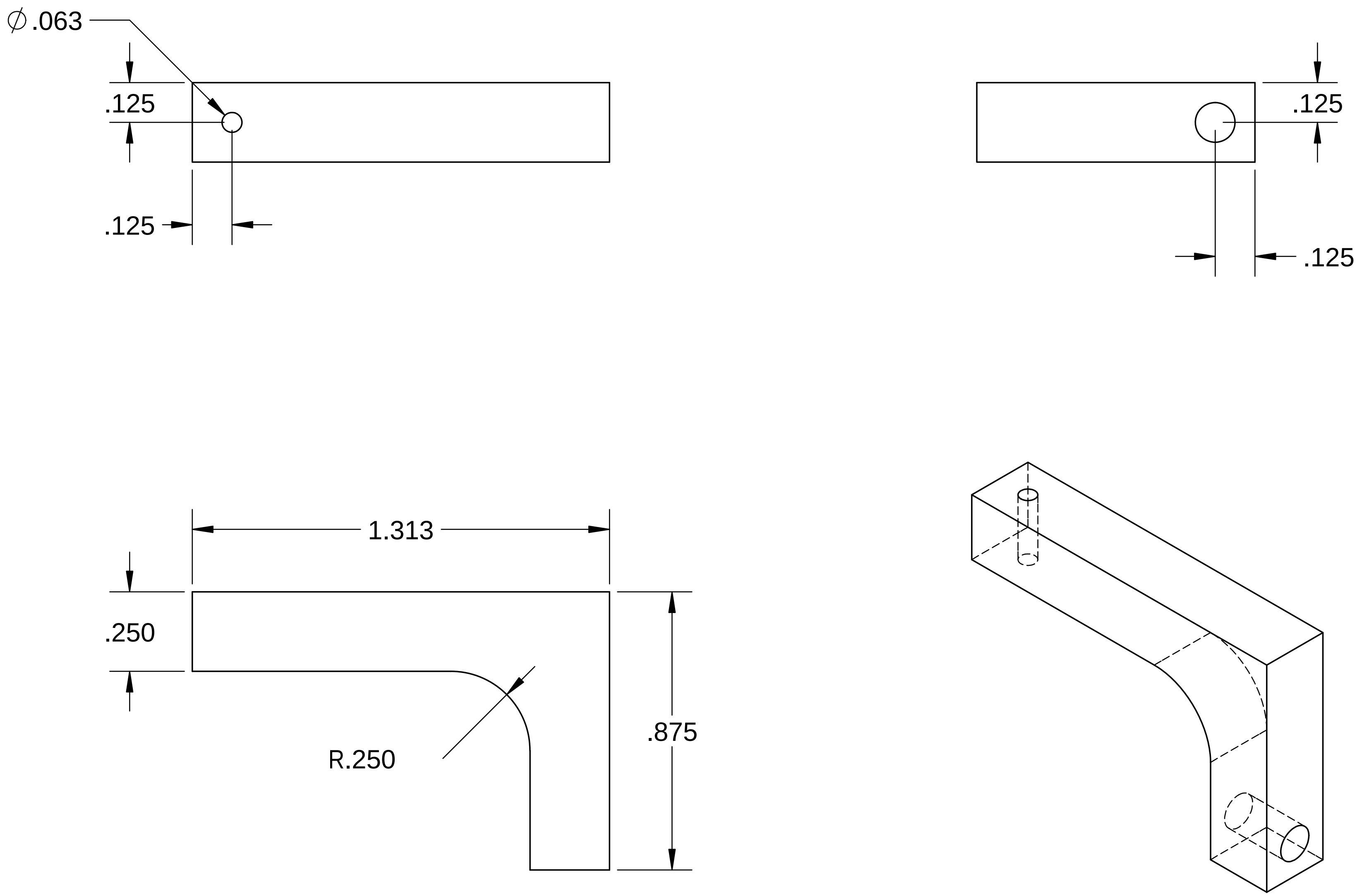

SIZE	Title
A	Part b

SCALE: 2:1 | DIMENSIONS ARE IN INCHES

5 4 3 2 1

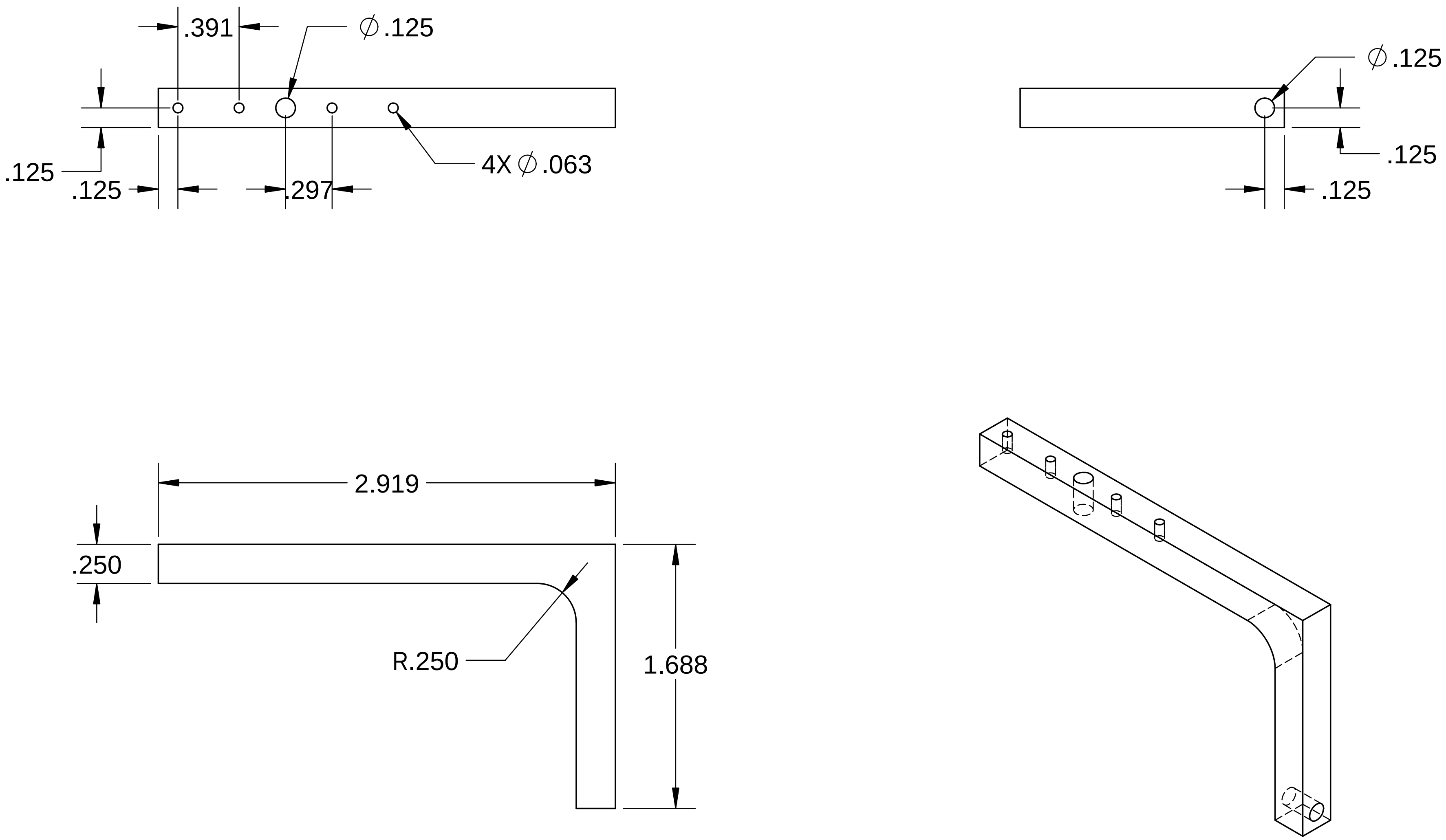

SIZE	Title
A	Part c
SCALE: 1:1	DIMENSIONS ARE IN INCHES

5 4 3 2 1

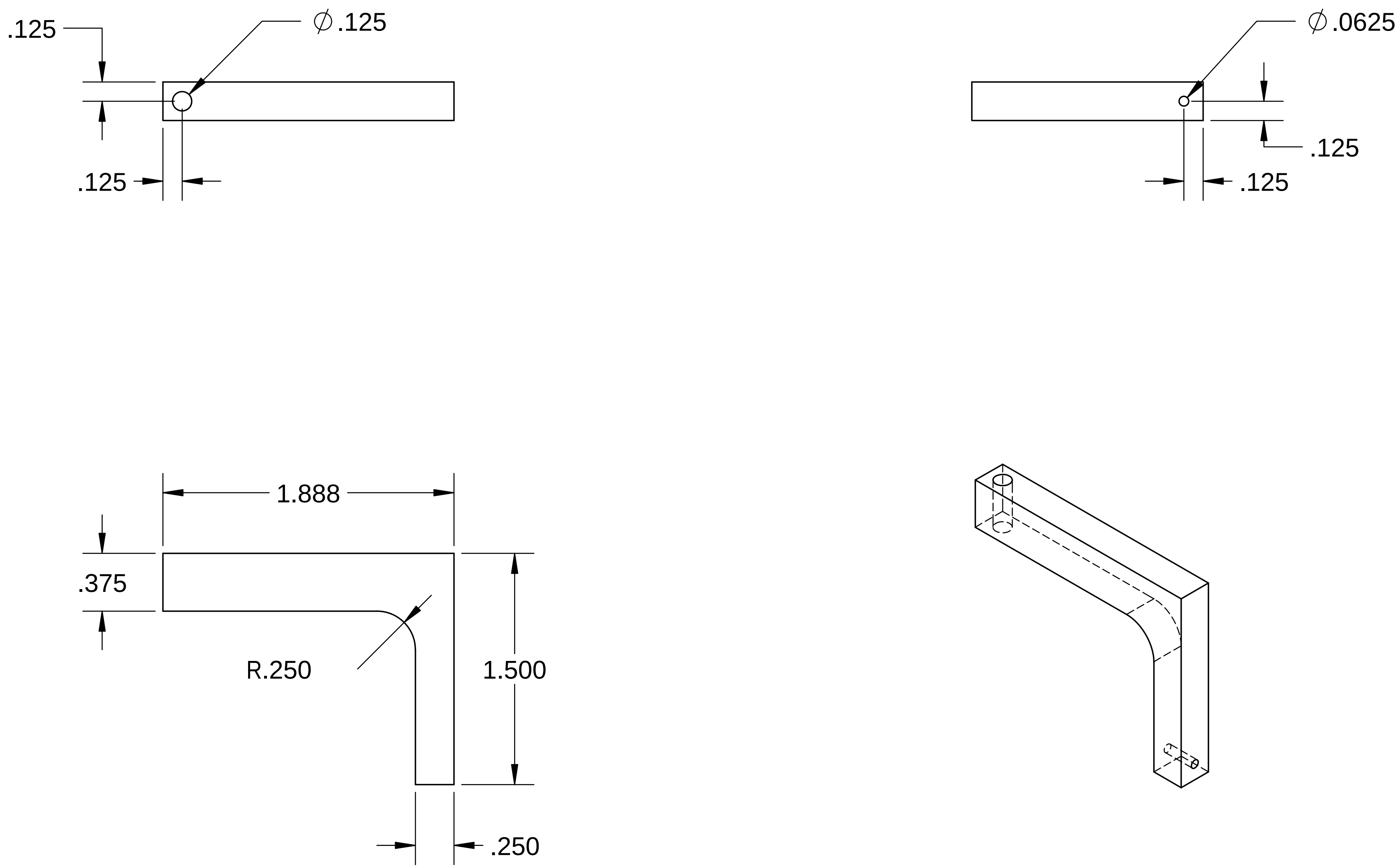

SIZE	Title
A	Part d
SCALE: 1:1	DIMENSIONS ARE IN INCHES

5 4 3 2 1

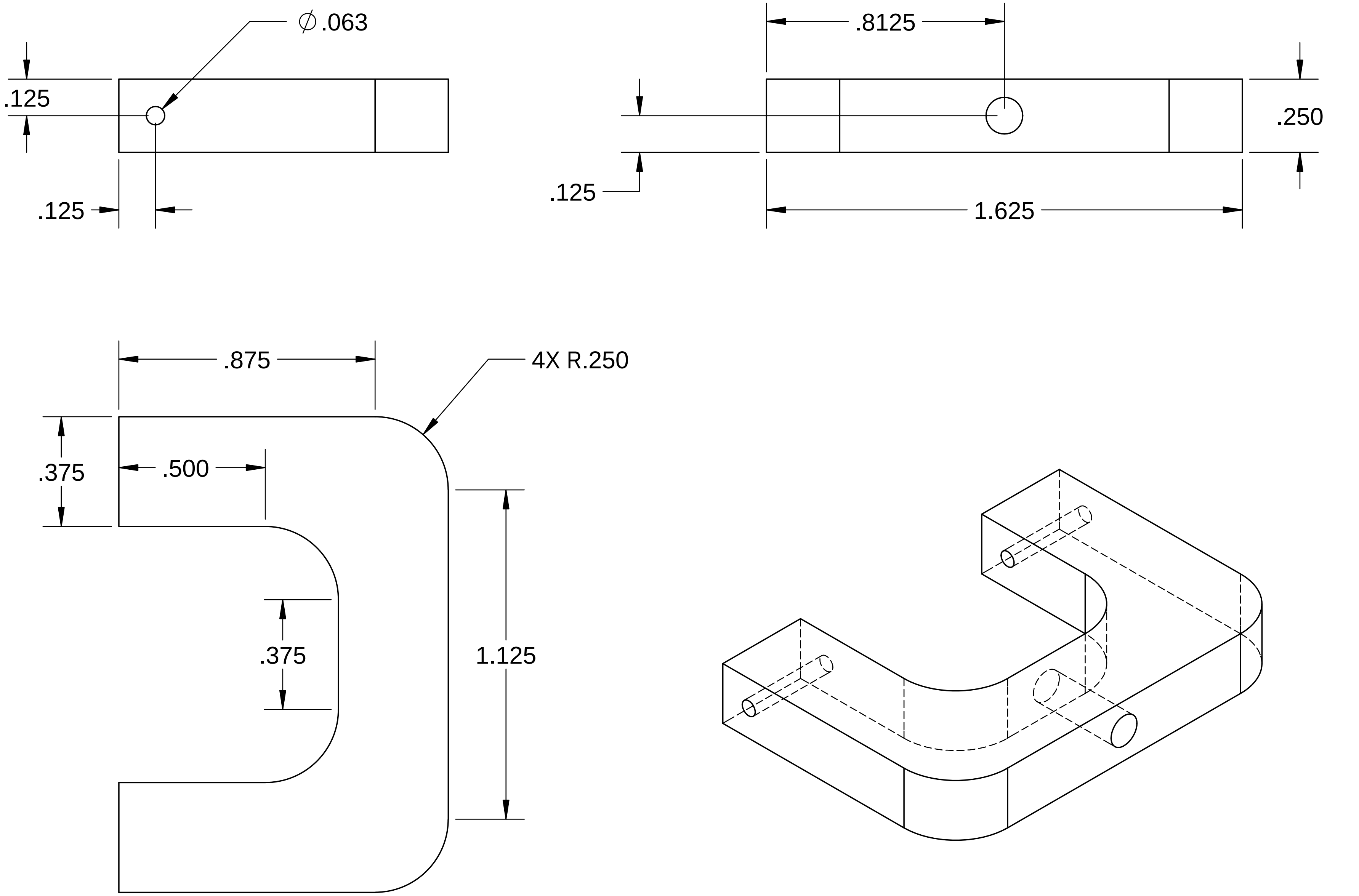

SIZE **A**

Title

Part e

SCALE: 2:1

DIMENSIONS ARE IN INCHES

5 4 3 2 1

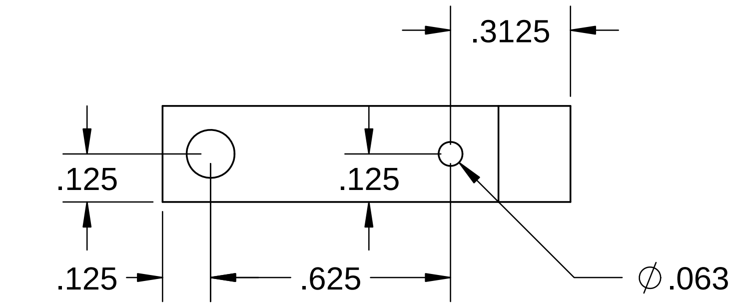

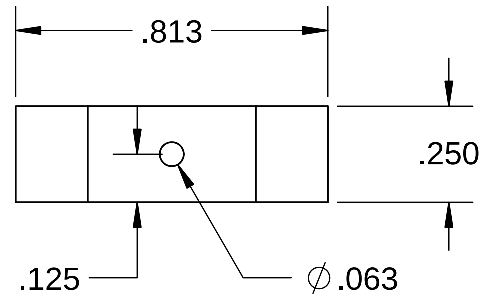

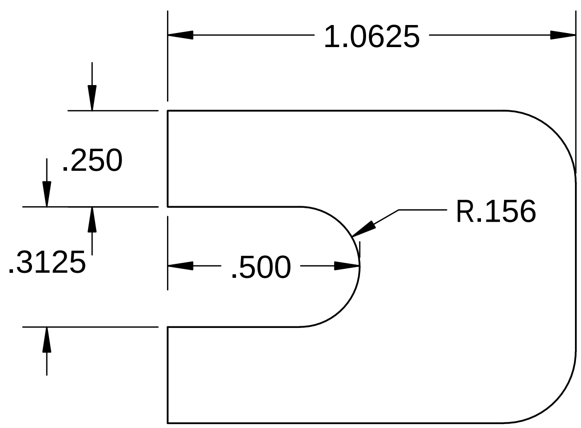

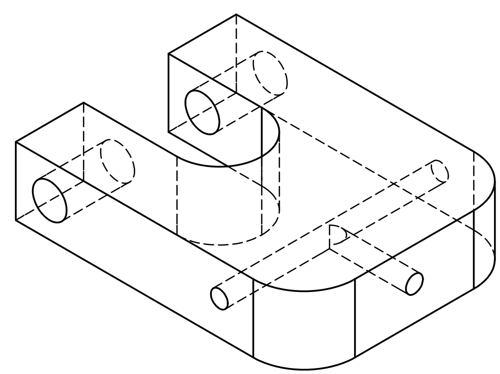

SIZE	Title
A	Part f
SCALE: 2:1	DIMENSIONS ARE IN INCHES

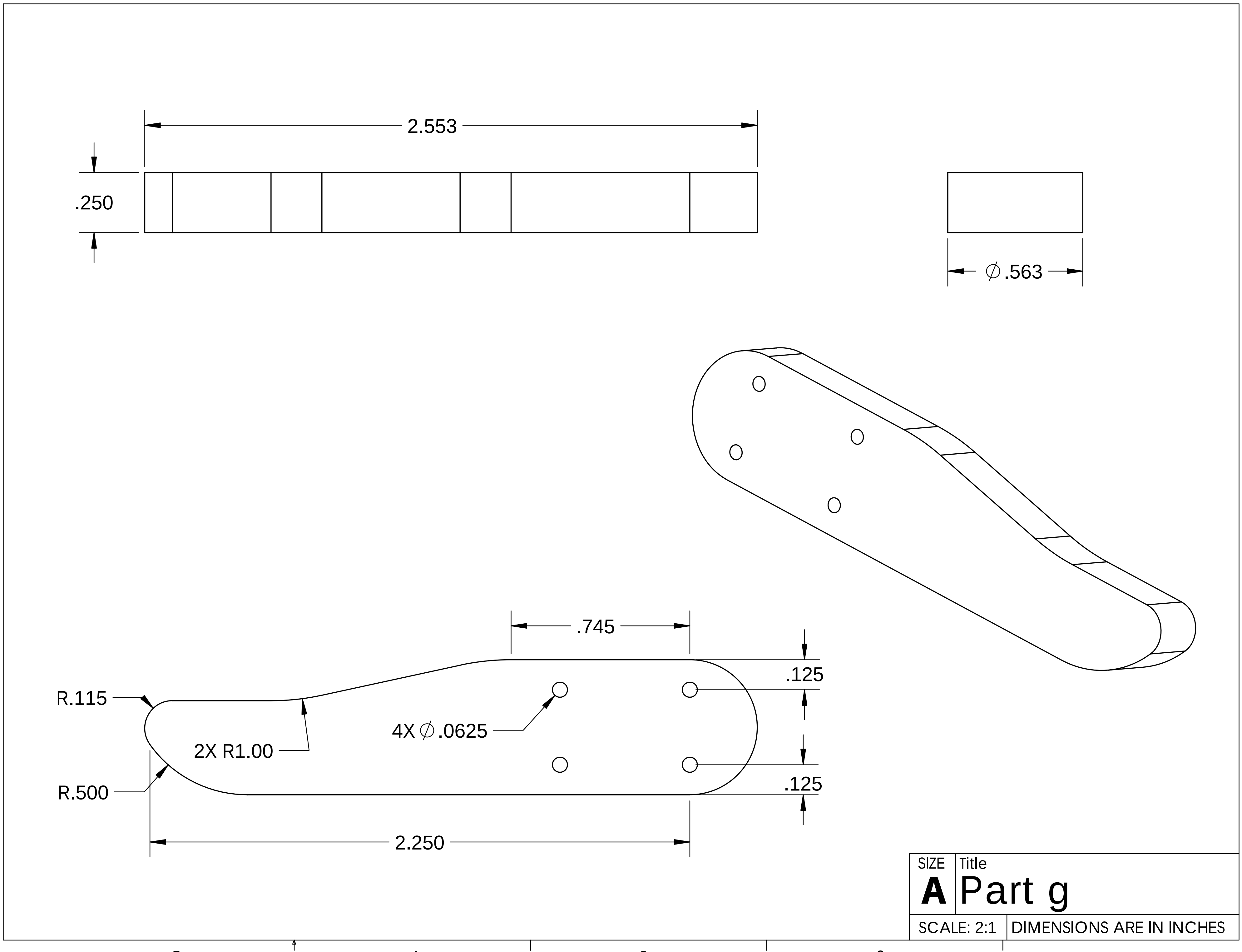

SIZE	Title
A	Part g
SCALE: 2:1	DIMENSIONS ARE IN INCHES

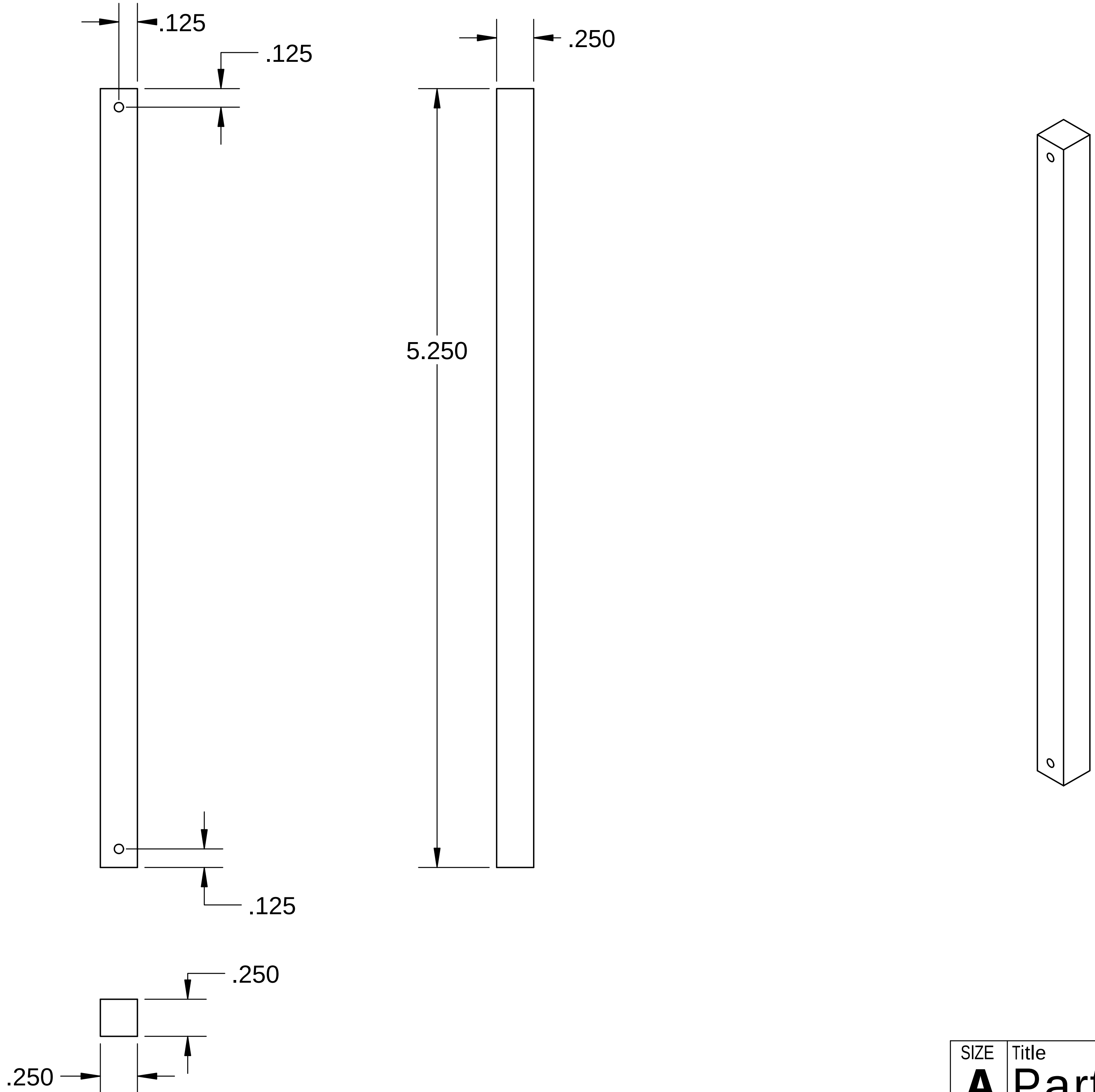

SIZE	Title
A	Part h
SCALE: 1:1	DIMENSIONS ARE IN INCHES

5 4 3 2 1

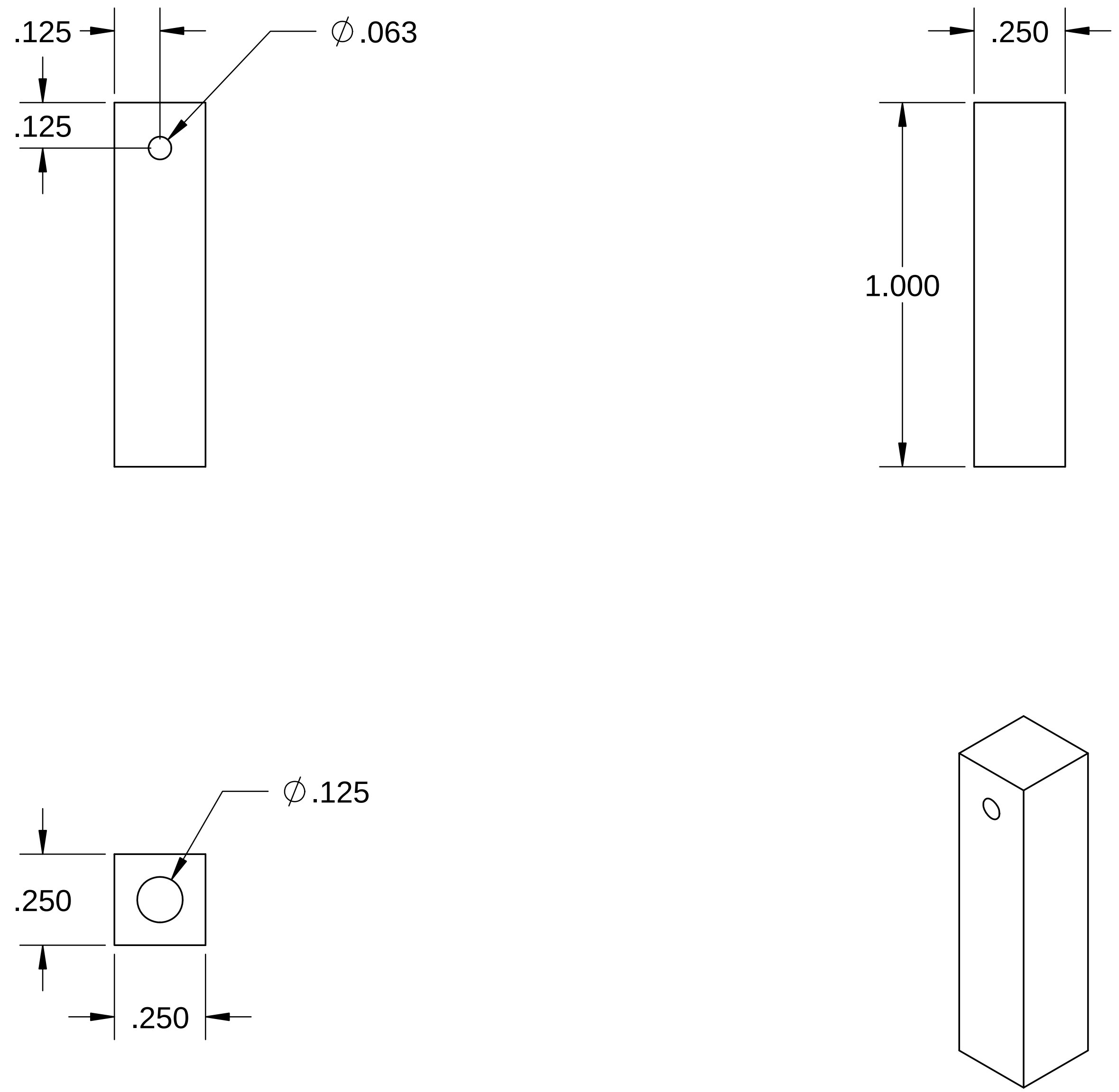

SIZE	Title
A	Part ia
SCALE: 2:1	DIMENSIONS ARE IN INCHES

5 4 3 2 1

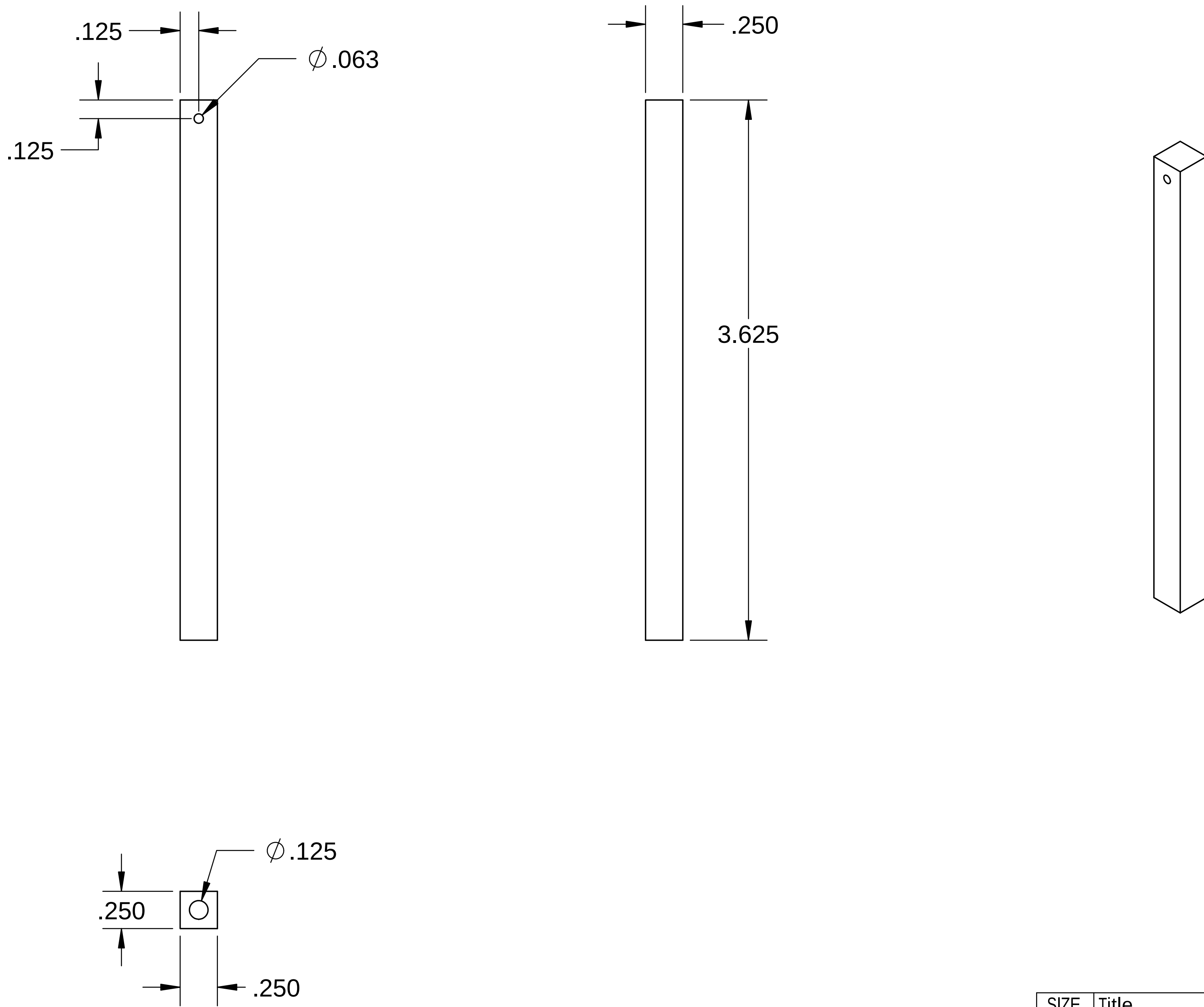

SIZE	Title
A	Part ib
SCALE: 1:1	DIMENSIONS ARE IN INCHES

5 4 3 2 1

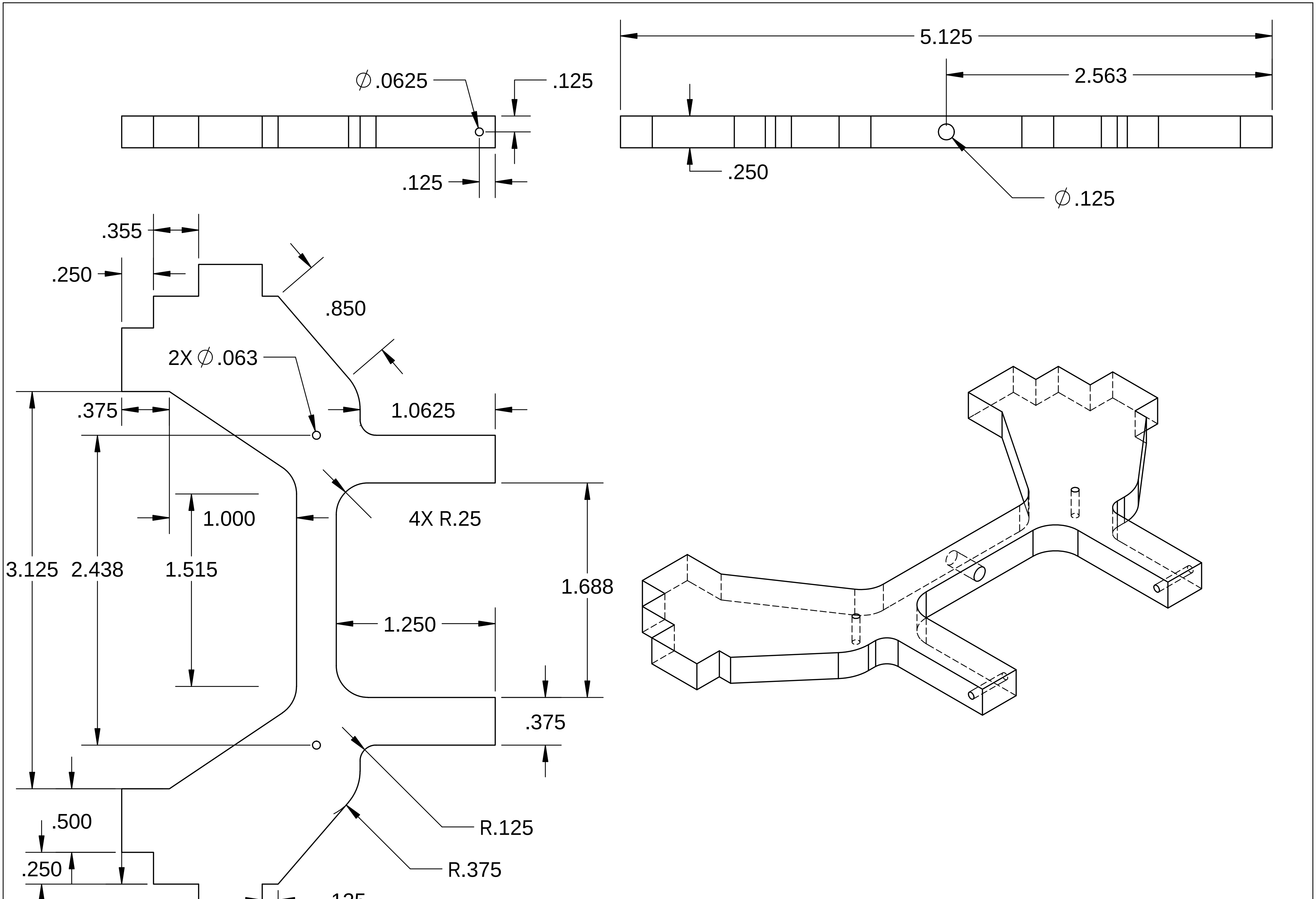

SIZE	Title
A	Leg Frame
SCALE: 1:1	DIMENSIONS ARE IN INCHES

5 4 3 2 1

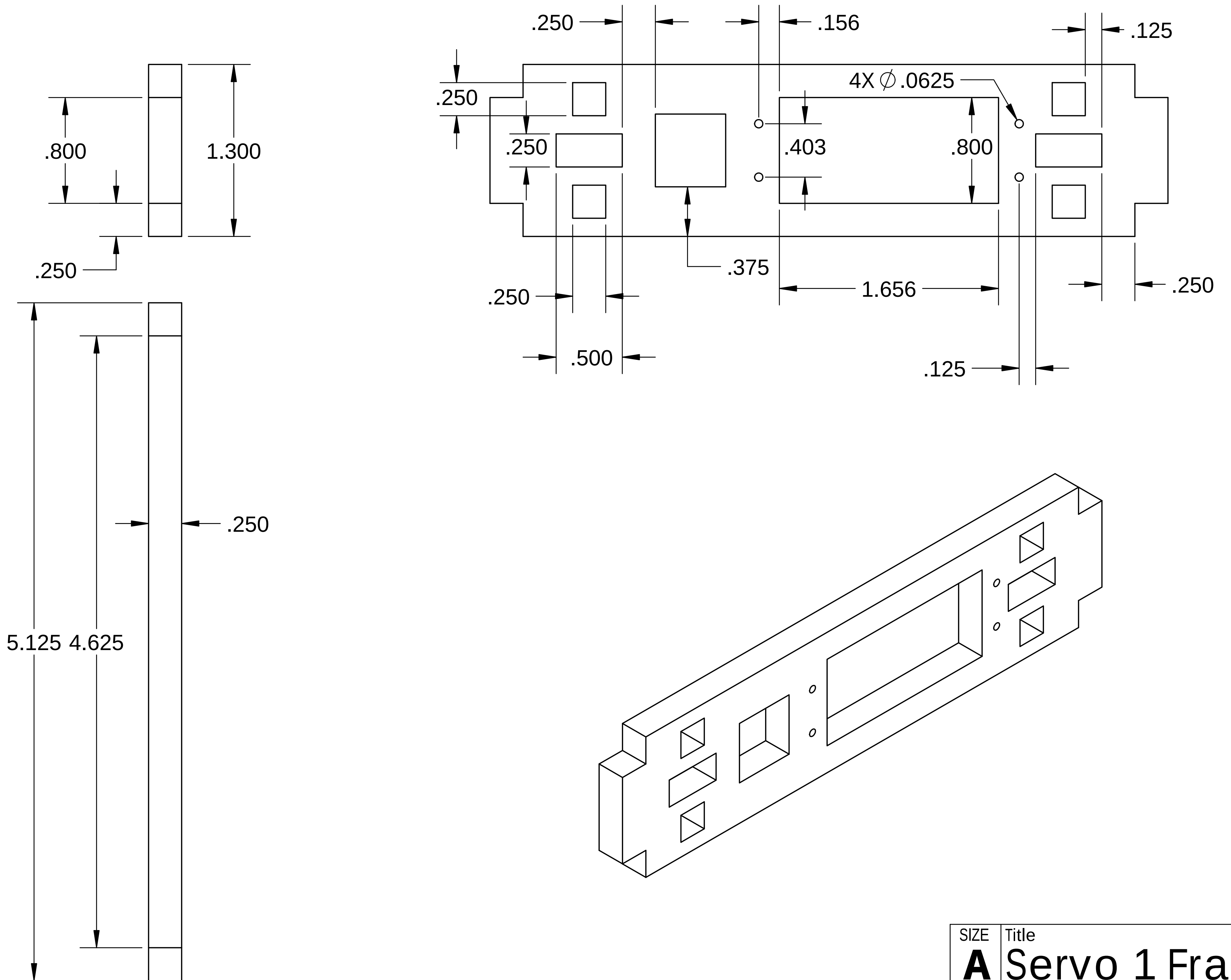

SIZE	Title
A	Servo 1 Frame
SCALE: 1:1	DIMENSIONS ARE IN INCHES

5 4 3 2 1

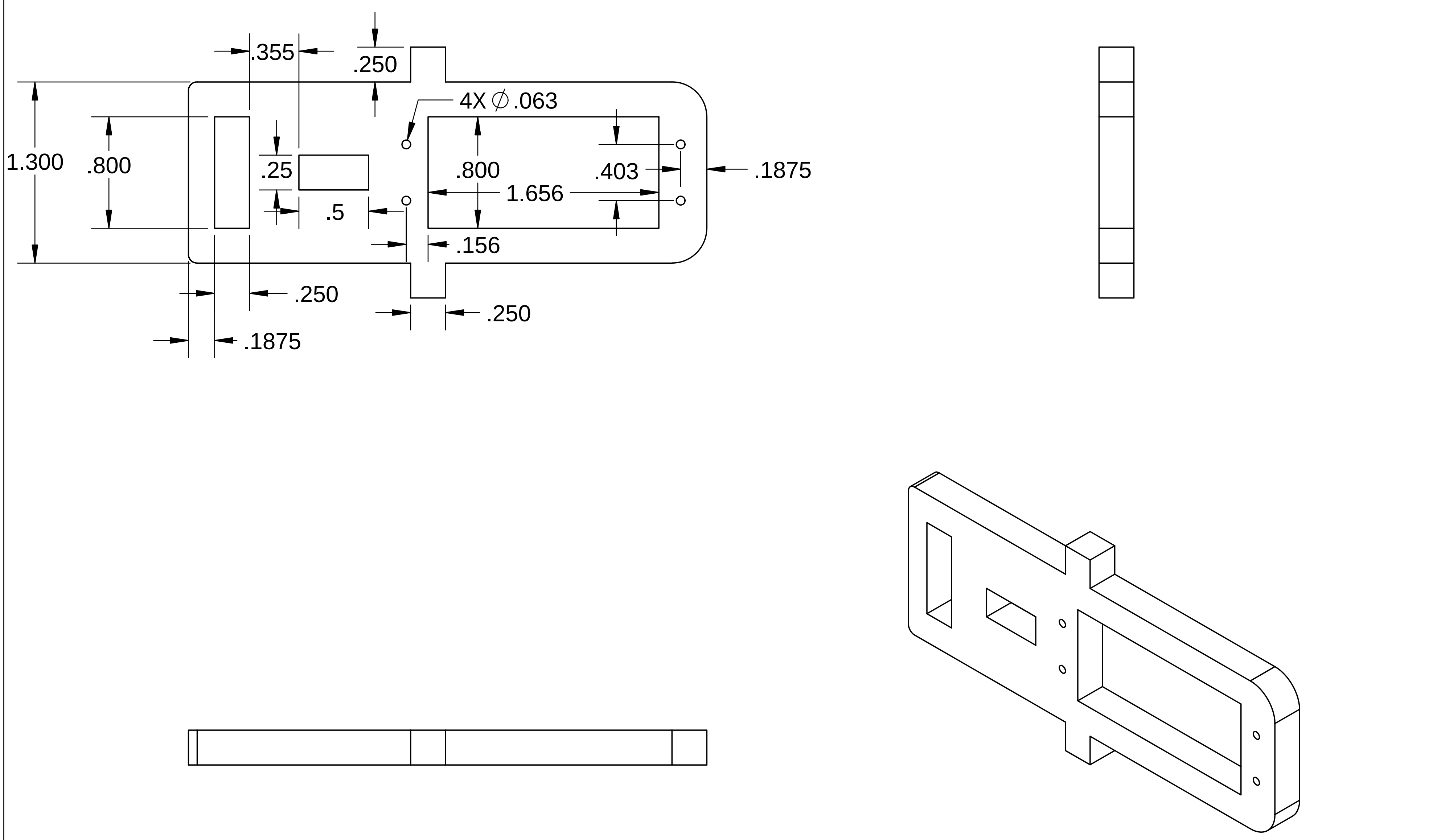

SIZE	Title
A	Servo 2&3 Frame
SCALE: 1:1	DIMENSIONS ARE IN INCHES

5 4 3 2 1

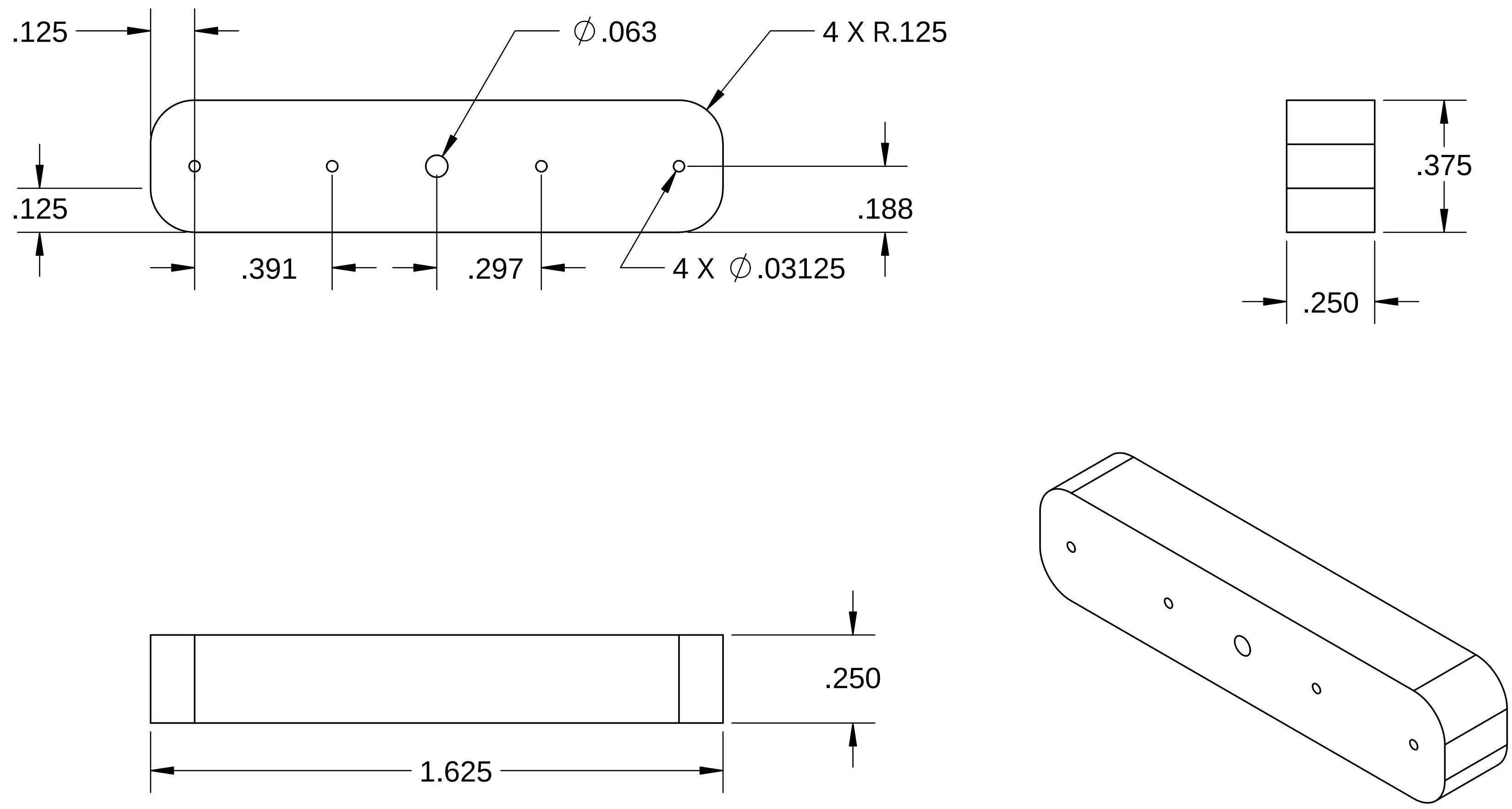

SIZE A | Title HornAdapter

SCALE: 2:1 | DIMENSIONS ARE IN INCHES

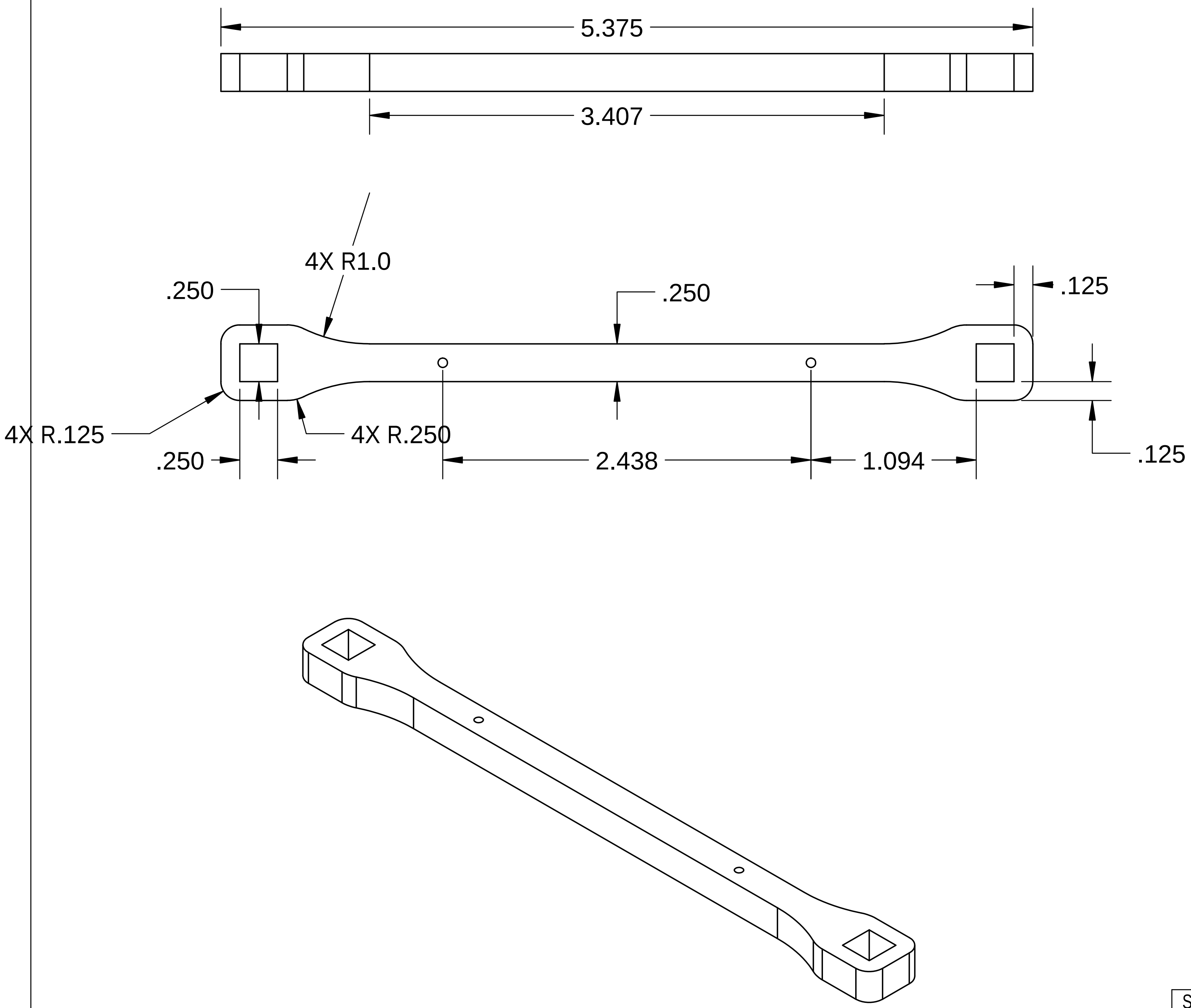

SIZE	Title
A	Frame Brace 1
SCALE: 1:1	DIMENSIONS ARE IN INCHES

5 4 3 2 1

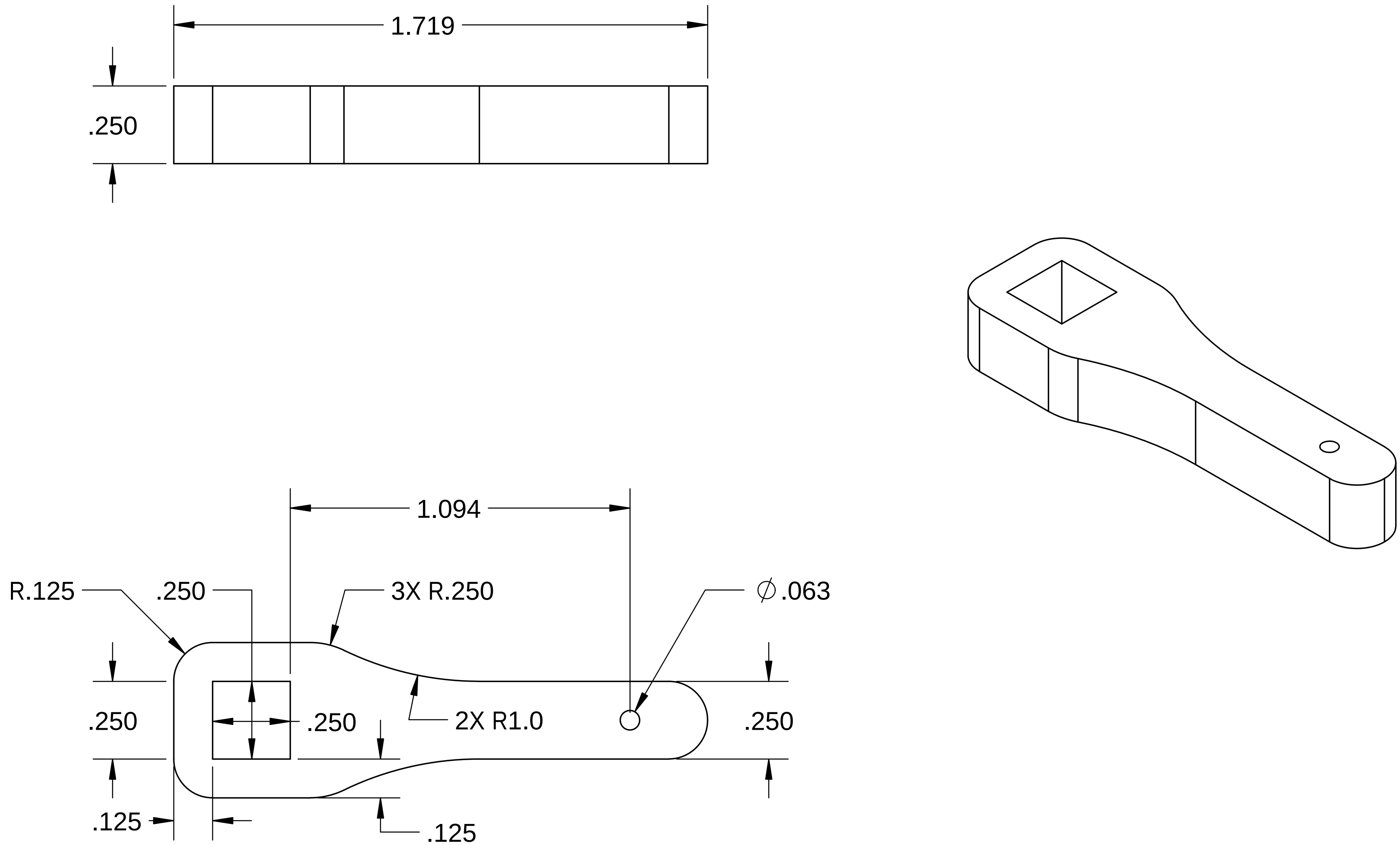

5 4 3 2 1

SIZE	Title
A	Frame Brace 2
SCALE: 2:1	DIMENSIONS ARE IN INCHES

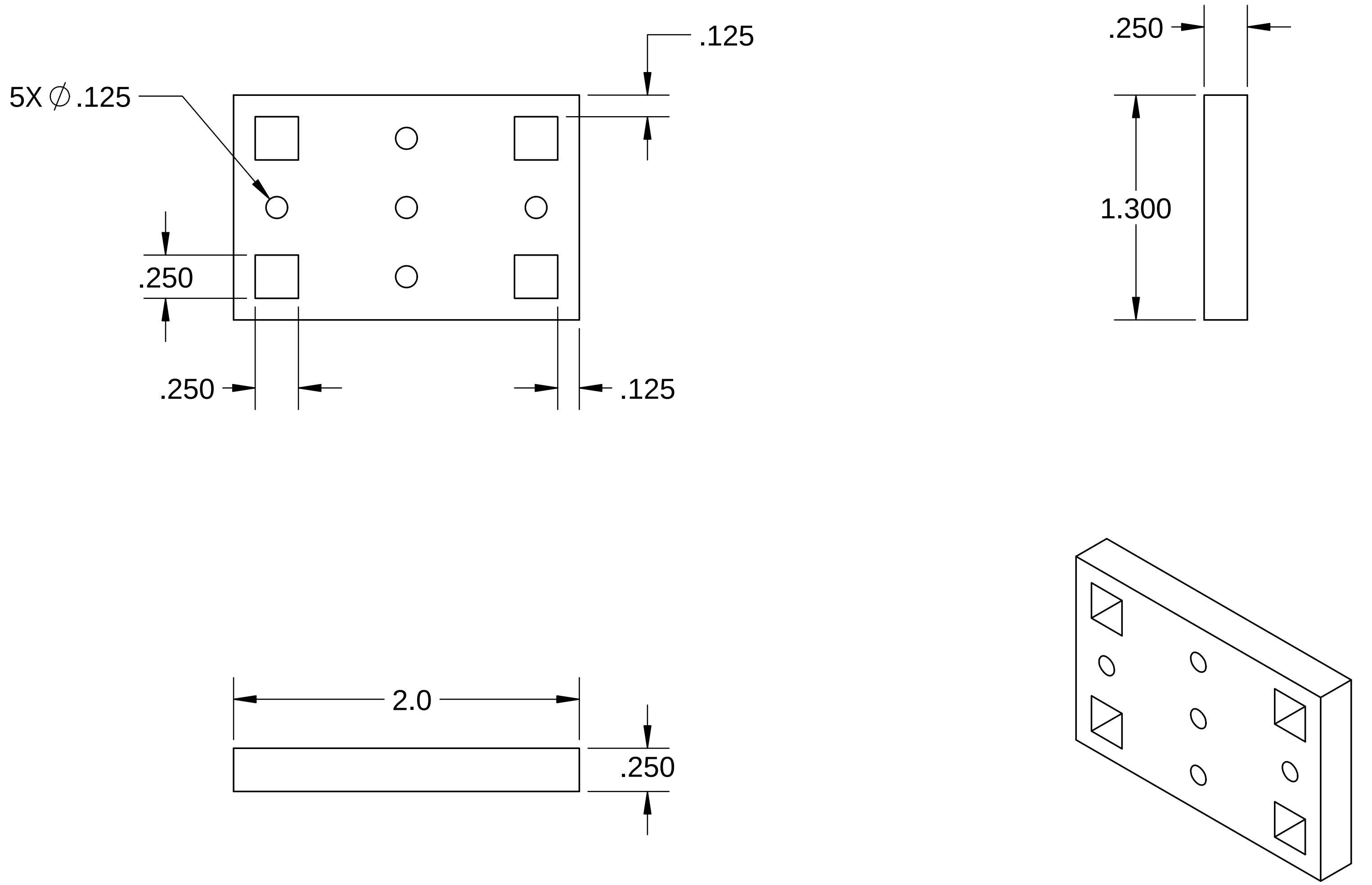

SIZE	Title
A	Frame End
SCALE: 1:1	DIMENSIONS ARE IN INCHES

5 4 3 2 1

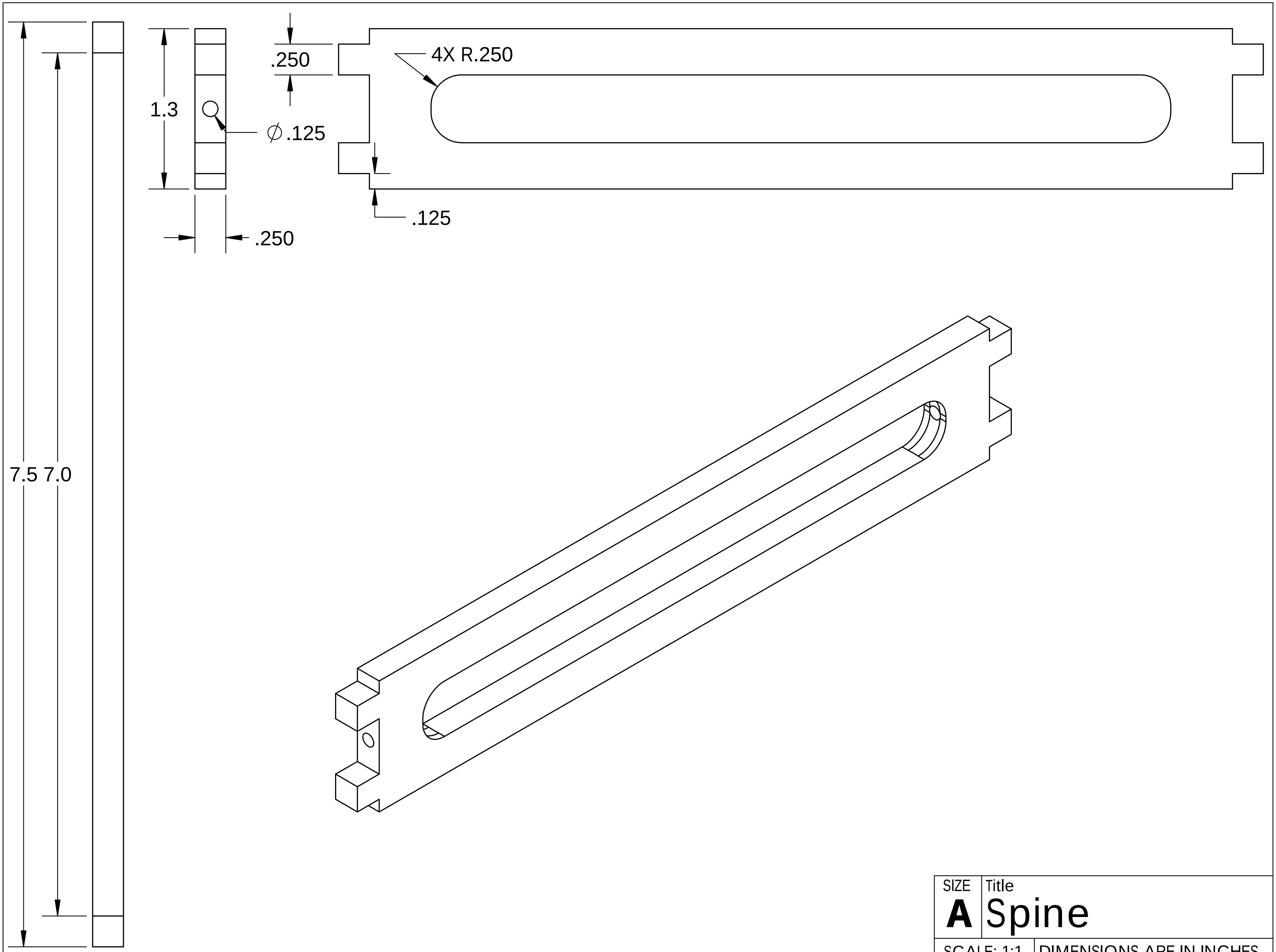

SIZE	Title
A	Spine
SCALE: 1:1	DIMENSIONS ARE IN INCHES

5 4 3 2 1

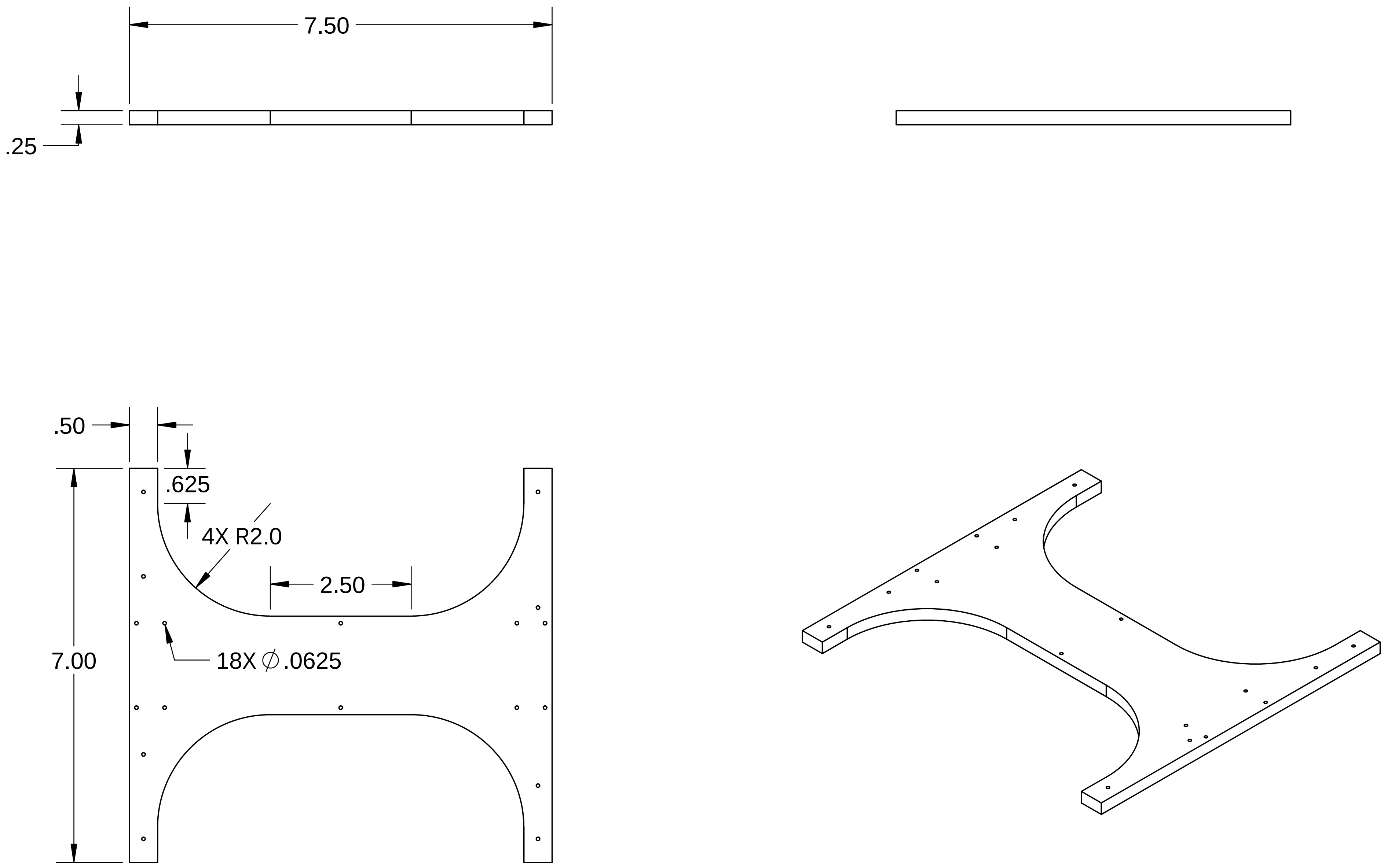

SIZE	Title
A	Support Plate
SCALE: 1:2.5	DIMENSIONS ARE IN INCHES

Appendix B

System Equations

The mathematics were done in Mathematica and a printout is included in this section.

Initialization

```
Clear["Global`*"]
Needs["PlotLegends`"]
```

The Rotation matrices are used to transfer the rotated frame to the fixed frame.
The Rotation Inverse (RI) matrices are used to transfer the fixed frame to the rotating frame.

$$\text{R1}[\alpha\_] := \begin{pmatrix} 1 & 0 & 0 \\ 0 & \text{Cos}[\alpha] & -\text{Sin}[\alpha] \\ 0 & \text{Sin}[\alpha] & \text{Cos}[\alpha] \end{pmatrix} \text{(*1st axis constant*)}$$

$$\text{R2}[\alpha\_] := \begin{pmatrix} \text{Cos}[\alpha] & 0 & \text{Sin}[\alpha] \\ 0 & 1 & 0 \\ -\text{Sin}[\alpha] & 0 & \text{Cos}[\alpha] \end{pmatrix} \text{(*2nd axis constant*)}$$

$$\text{R3}[\alpha\_] := \begin{pmatrix} \text{Cos}[\alpha] & -\text{Sin}[\alpha] & 0 \\ \text{Sin}[\alpha] & \text{Cos}[\alpha] & 0 \\ 0 & 0 & 1 \end{pmatrix} \text{(*3rd axis constant*)}$$

Make SURE that the rotation matrices are used as show:
a=R.b
Use the RHR for angle direction

Part Vectors and Simplifications

```
values = {
   x1 → 1,
   x2 → 1.4375,
   a2 → 1.4375,
   a3 → 0.96875,
   b1 → 1.0625,
   b3 → 0.96875,
   c1 → 1.98125,
   c2 → 1.4375,
   d1 → 1.98125,
   d3 → 1.1875,
   e1 → 1,
   f1 →  0.625,
   fp1 → 1.0625,
   g1 → 2.25,
   ia → 1.1875,
   ib → 3.8125,
   h → 5
  };
```

```
ra = {0, -a2, a3};
rb = {b1, 0, -b3};
rc = {c1, c2, 0};
rd = {-d1, 0, -d3};
re = {e1, 0, 0};
rfh = {f1, 0, 0};
rfb = {fp1, 0, 0};
rg = {g1, 0, 0};(*The "foot"*)
rgh = {g1 - f1, 0, 0};(*The "toes"*)
rh = {0, 0, -h};
rid = {0, 0, -ia};
rdg = {0, 0, -ib};
rx1 = {0, 0, 0};(*Link 0*)
rx2 = {x1, -x2, 0};(*Link 1*)
rx3 = {x1, x2, 0};(*Link 2*)
```

Simplifications:

$x_1 == e_1$
$x_2 == a_2 == c_2$
$a_3 == b_3$
$c_1 == d_1$
$b_1 == f_{\mathrm{p1}}$
$i_a == d_3$
$i_b == h - i_a$

```
Simple = {
    x1 → e1,
    a2 → x2,
    c2 → x2,
    a3 → b3,
    c1 → d1,
    fp1 → b1,
    d3 → ia
   };
```

Angles:

$\phi_{\mathrm{ab}} = r_a \angle r_b$
$\phi_{\mathrm{bf}} = r_b \angle r_f$

$\phi_{\mathrm{cd}} = r_c \angle r_d$
$\phi_{\mathrm{di}} = r_d \angle r_{\mathrm{ia}}$

$\theta_1 = r_{\mathrm{x1}} \angle r_e$
$\theta_2 = r_{\mathrm{x2}} \angle r_c$
$\theta_3 = r_{\mathrm{x3}} \angle r_a$

$\alpha = \hat{e}_1 \angle \hat{f}_1 = \hat{e}_1 \angle \hat{g}_1$

$\beta = \hat{e}_3 \angle \hat{f}_3 = \hat{e}_3 \angle \hat{g}_3$

$\gamma = \hat{e}_3 \angle \hat{i}_3 = \hat{e}_3 \angle \hat{h}_3 = \theta_1$

Actuator Equations

To solve for the static torque requirements of each actuator the relation between the end effector and the actuators. Noting that each actuator is primarily controlling one range of motion the static analysis is divided into three segments, one for each actuator.

To apply this assumption when analyzing one actuator the angles of the other actuators are set to zero. That is to say the mechanism is put into the standard anatomical position and then one actuator will be free to move at a time.

Using the following two equations several simplifications to the internal angles can be applied. These equations are derived in the Section Closed Loops

```
Tan[β] == Cos[θ1] Tan[θ2]
Tan[α] == Sec[θ1] Tan[θ3]
```

- **Actuator 1**

Let $\theta_2 == \theta_3 == 0$
Then $\alpha == \beta == 0$
Forcing the d, e, f, g, h, and i reference frames to be identical.

```
ServoArm1 = R1[θ1].(re + rdg + rid + rg);
ServoArm1 = ServoArm1 /. Simple /. -ia - ib → -h
```

```
{e1 + g1, h Sin[θ1], -h Cos[θ1]}
```

- **Actuator 2**

Let $\theta_1 == \theta_3 == 0$
Then $\alpha == 0$ and $\beta == \theta_2$
Forcing the c, d, h, and i reference frames to be identical.
Note that the angle between the i and g reference frames is $-\beta$.

```
ServoArm2 = R2[θ2].(rc + rd + rdg + R2[-β].rg)
ServoArm2 = ServoArm2 /. Simple /. -ia - ib → -h /. β → θ2
ServoArm2 = ServoArm2 // Expand // TrigFactor
```

```
{Cos[θ2] (c1 - d1 + Cos[β] g1) + Sin[θ2] (-d3 + Sin[β] g1 - ib),
 c2, -Sin[θ2] (c1 - d1 + Cos[β] g1) + Cos[θ2] (-d3 + Sin[β] g1 - ib)}
```

```
{Cos[θ2]^2 g1 + Sin[θ2] (-h + Sin[θ2] g1),
 x2, -Cos[θ2] Sin[θ2] g1 + Cos[θ2] (-h + Sin[θ2] g1)}
```

```
{-h Sin[θ2] + g1, x2, -h Cos[θ2]}
```

- **Actuator 3**

Let $\theta_1 == \theta_2 == 0$
Then $\alpha == \theta_3$ and $\beta == 0$ and $\phi_{ab} == \phi_{bf} == 0$

The third actuator has additional kinematics to consider. Because the linkages forms a four bar mechanism the links transfer power (in theory) perfectly for this actuator. Performing a simple torque analysis we see the following: $F_f * f_{1+} = F_g * g_1$

To solve for the torque required by the servo the force needed to hold link-g, given link-h and link-i are locked, is determined. f_g is related to f_f where f_f is the force needed to hold link-f in place. f_f

is then related to the a reference frame. Given that the system starts in the standard anatomical position the a, b, and f reference frames are identical giving $f_a == f_f$ where f_a is the force f_f in the a reference frame.

The final assumption is that the component of f_a along the common first axis of the g, f, a, and b reference frames has no effect on the servo and is completely converted to torque on the second actuator or as a perpendicular force applied to the joints.

$$\mathbf{f}_{\mathbf{g}\alpha} = \mathbf{R2}[-\alpha].\{\mathbf{0}, \mathbf{0}, \mathbf{PerLegWeight}\} \text{ /. } \alpha \to \theta_3$$

$$\mathbf{f}_{\mathbf{f}} = \frac{\mathbf{g}_1}{\mathbf{f}_{\mathbf{p1}}} \mathbf{f}_{\mathbf{g}\alpha} \text{ /. values(*Ummm... Get the direction right*)}$$

$$\mathbf{f}_{\mathbf{a}} = \{\mathbf{0}, \mathbf{0}, \mathbf{f}_{\mathbf{f}}[[\mathbf{3}]]\} \text{ /. } \alpha \to \theta_3$$

$$\{-\text{PerLegWeight}\,\text{Sin}[\theta_3], 0, \text{PerLegWeight}\,\text{Cos}[\theta_3]\}$$

$$\{-2.11765\,\text{PerLegWeight}\,\text{Sin}[\theta_3], 0, 2.11765\,\text{PerLegWeight}\,\text{Cos}[\theta_3]\}$$

$$\{0, 0, 2.11765\,\text{PerLegWeight}\,\text{Cos}[\theta_3]\}$$

$$\mathbf{Link}_{\mathbf{ab}} = (\mathbf{r}_{\mathbf{a}} + \mathbf{R3}[\phi_{\mathbf{ab}}].\mathbf{r}_{\mathbf{b}})$$

$$\mathbf{Link}_{\mathbf{ab}} = \mathbf{Link}_{\mathbf{ab}} \text{ /. } \{\phi_{\mathbf{ab}} \to \mathbf{0}\} \text{ /. values}$$

$$(*\mathbf{Link}_{\mathbf{ab}}=\mathbf{Link}_{\mathbf{ab}}\{1,0,0\}*)$$

$$(*\text{There is an } \mathbf{a}_2 \text{ part but it is invalid from this analysis}*)$$

$$\{\text{Cos}[\phi_{ab}]\,b_1, -a_2 + \text{Sin}[\phi_{ab}]\,b_1, a_3 - b_3\}$$

$$\{1.0625, -1.4375, 0.\}$$

$$\tau_3 = \mathbf{Link}_{\mathbf{ab}} \times \mathbf{f}_{\mathbf{a}}$$

$$\{0. - 3.04412\,\text{PerLegWeight}\,\text{Cos}[\theta_3], 0. - 2.25\,\text{PerLegWeight}\,\text{Cos}[\theta_3], 0.\}$$

The torque along the X_2 axis is the torque required by the third servo to statically hold link-g.

- **Actuator Torques**

All values are based on units of ounces and/or inches

```
ServoMaxTorque = 180;
SingleServoWeight = 2.1;
ServoWeight = SingleServoWeight * 12;
FrameWeight = ServoWeight / 3;
BatteryWeight = 10;(*Typical of Li-Ion needed for 12 0.4 Amp servos*)
(*LegWeight is the weight of the leg that the servo must overcome*)
LegWeight = 3 + 3;(*Weight of plastic + Estimated weight of metal parts*)
ControlWeight = 5;(*This is hopefully way overkill*)
Payload = 16;(*Desired Minimum load capacity*)
```

```
Weight = (ServoWeight + BatteryWeight + ControlWeight + FrameWeight + Payload)
(*Estimated robot weight*)
PLWA = PerLegWeight → Ceiling[Weight / 3](*Weight on stationary legs*)
PLWB = PerLegWeight → Ceiling[LegWeight](*Weight of moving leg*)
```

```
64.6
```

```
PerLegWeight → 22
```

```
PerLegWeight → 6
```

The force applied to the end effector by the ground is in X-Y-Z coordinates. Assuming The X-Y-Z frame and the X frame are identical the force must be converted from X_3 to be in terms of g

```
fgβ = R2[0].{0, 0, PerLegWeight} /. β → θ2
fgγ = R1[-γ].{0, 0, PerLegWeight} /. γ → θ1
```

```
{0, 0, PerLegWeight}
```

```
{0, PerLegWeight Sin[θ1], PerLegWeight Cos[θ1]}
```

```
(*Solving for the torques at long last*)
τ1 = ServoArm1 × fgγ // Simplify
τ2 = ServoArm2 × fgβ // Simplify
τ3
```

```
{h PerLegWeight Sin[2 θ1],
 -PerLegWeight Cos[θ1] (e1 + g1), PerLegWeight Sin[θ1] (e1 + g1)}
```

```
{PerLegWeight x2, PerLegWeight (h Sin[θ2] - g1), 0}
```

```
{0. - 3.04412 PerLegWeight Cos[θ3], 0. - 2.25 PerLegWeight Cos[θ3], 0.}
```

```
τ1 /. PLWB
Servo1FreeTorque = %[[1]] /. values;
τ2 /. PLWB
Servo2FreeTorque = %[[2]] /. values;
```

```
{6 h Sin[2 θ1], -6 Cos[θ1] (e1 + g1), 6 Sin[θ1] (e1 + g1)}
```

```
{6 x2, 6 (h Sin[θ2] - g1), 0}
```

```
τ1 /. PLWA
Servo1HoldTorque = %[[1]] /. values;
τ2 /. PLWA
Servo2HoldTorque = %[[2]] /. values;
τ3 /. PLWA
Servo3HoldTorque = %[[2]] /. values;
```

```
{22 h Sin[2 θ1], -22 Cos[θ1] (e1 + g1), 22 Sin[θ1] (e1 + g1)}
```

```
{22 x2, 22 (h Sin[θ2] - g1), 0}
```

```
{0. - 66.9706 Cos[θ3], 0. - 49.5 Cos[θ3], 0.}
```

Cos has a max at 0

Sin has a max at $\pi/2$

```
Servo1FreeTorque /. θ1 → π / 4
Servo2FreeTorque /. θ2 → π / 2
```

```
30
```

```
16.5
```

```
Servo3HoldTorque /. θ3 → 0
Servo2HoldTorque /. θ2 → π / 2
maxTorque = Servo1HoldTorque /. θ1 → π / 4
normTorque = Servo1HoldTorque /. θ1 → 15 Degree
```

-49.5

60.5

110

55

Because the analysis has been done for a static system a desired stall torque for the actuator should be 3 times the max torque from the analysis.

```
ServoMaxTorque / maxTorque // N
ServoMaxTorque / normTorque // N
```

1.63636

3.27273

End Effector Position

Given α, β, and γ the position of the end effector can be given in the x coordinate frame.

Given that f and g reference frames are identical they both transfer to the e reference frame using $R_2[\alpha]$

Solve for the end effector position relative to the hinge internal to the top of link-i_a, the mechanism pivot point. Ensure that the set of equations are in the X reference frame.

Path:

- Begin at the end of link-g
- From the end of link-g transfer to link-h
- From link-h transfer to the mechanism origin through f
- Translate the link origin from e to X

Math Trick:

By transforming link-g, link-h, and link-f into the e reference frame the resultant is found by simply adding vectors.

```
Pos = R1[γ].(R2[β].r_h + R2[α].r_fh + R2[α].r_gh) // Simplify
Pos // MatrixForm
```

$$\{-h\,\mathrm{Sin}[\beta] + \mathrm{Cos}[\alpha]\,g_1,\ \mathrm{Sin}[\gamma]\,(h\,\mathrm{Cos}[\beta] + \mathrm{Sin}[\alpha]\,g_1),\ -\mathrm{Cos}[\gamma]\,(h\,\mathrm{Cos}[\beta] + \mathrm{Sin}[\alpha]\,g_1)\}$$

$$\begin{pmatrix} -h\,\mathrm{Sin}[\beta] + \mathrm{Cos}[\alpha]\,g_1 \\ \mathrm{Sin}[\gamma]\,(h\,\mathrm{Cos}[\beta] + \mathrm{Sin}[\alpha]\,g_1) \\ -\mathrm{Cos}[\gamma]\,(h\,\mathrm{Cos}[\beta] + \mathrm{Sin}[\alpha]\,g_1) \end{pmatrix}$$

```
X1[α_, β_] := g1 Cos[α] - h Sin[β]
X2[α_, β_, γ_] := Sin[γ] (h Cos[β] + g1 Sin[α])
X3[α_, β_, γ_] := -Cos[γ] (h Cos[β] + g1 Sin[α])
```

```
X1[α, β]^2 + X2[α, β, γ]^2 + X3[α, β, γ]^2;
ArmLength = Sqrt[(% // Simplify)]
```

$$\sqrt{h^2 + 2\,h\,\mathrm{Sin}[\alpha - \beta]\,g_1 + g_1^2}$$

```
ArmLength /. α → β
ArmLength /. α → -β // Expand
```

$$\sqrt{h^2 + g_1^2}$$

$$\sqrt{h^2 - 2\,h\,\mathrm{Sin}[2\,\beta]\,g_1 + g_1^2}$$

```
ArmLength /. α → 0 ° /. β → 0 ° /. values // N
```

5.48293

```
Plot3D[ArmLength /. values, {α, -π / 2, π / 2}, {β, -π / 2, π / 2},
 AxesLabel → {"α (rad)", "β (rad)", "Length of leg (in)"}]
```

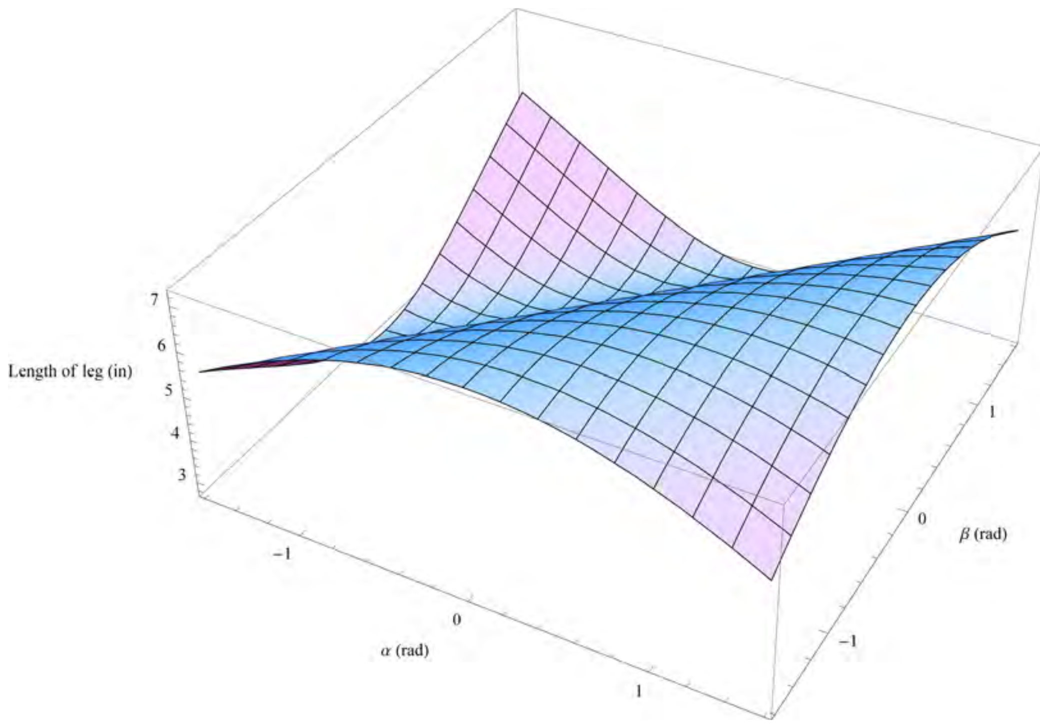


```
p = Pos /. values
```

```
{2.25 Cos[α] - 5 Sin[β],
 (5 Cos[β] + 2.25 Sin[α]) Sin[γ], -Cos[γ] (5 Cos[β] + 2.25 Sin[α])}
```

```
Plot3D[p[[1]] /. γ → 0, {α, -π / 2, π / 2}, {β, -π / 2, π / 2},
 AxesLabel → {"α (rad)", "β (rad)", "X₁ pos (in)"}]
```

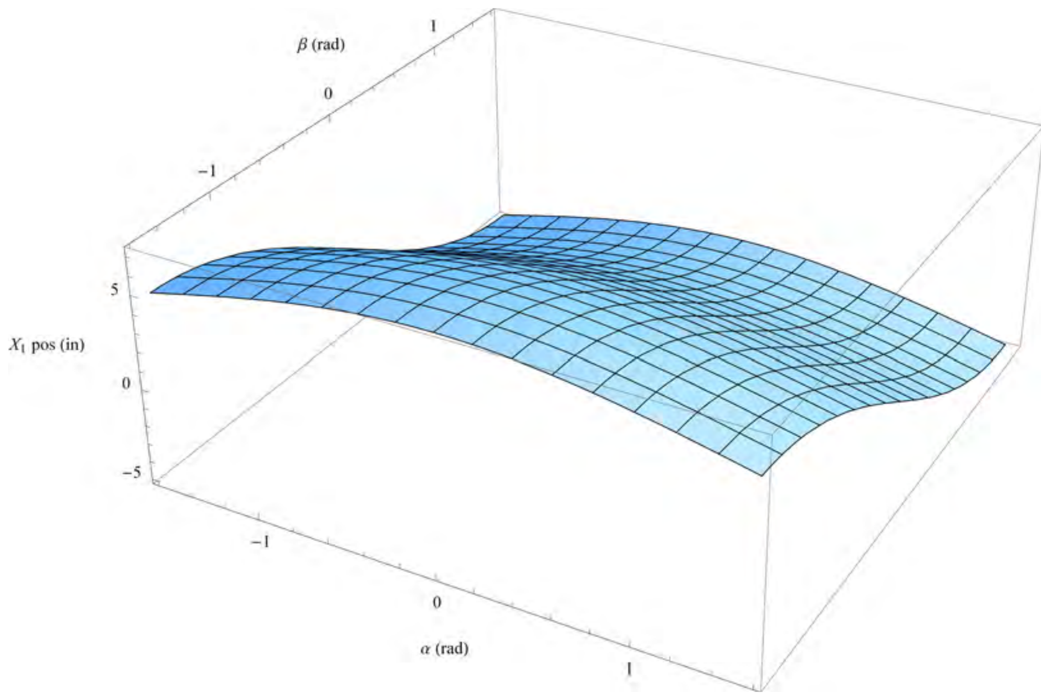


```
Plot3D[p[[3]] /. γ → 0, {α, -π / 2, π / 2}, {β, -π / 2, π / 2},
 AxesLabel → {"α (rad)", "β (rad)", "X₃ pos (in)"}]
```

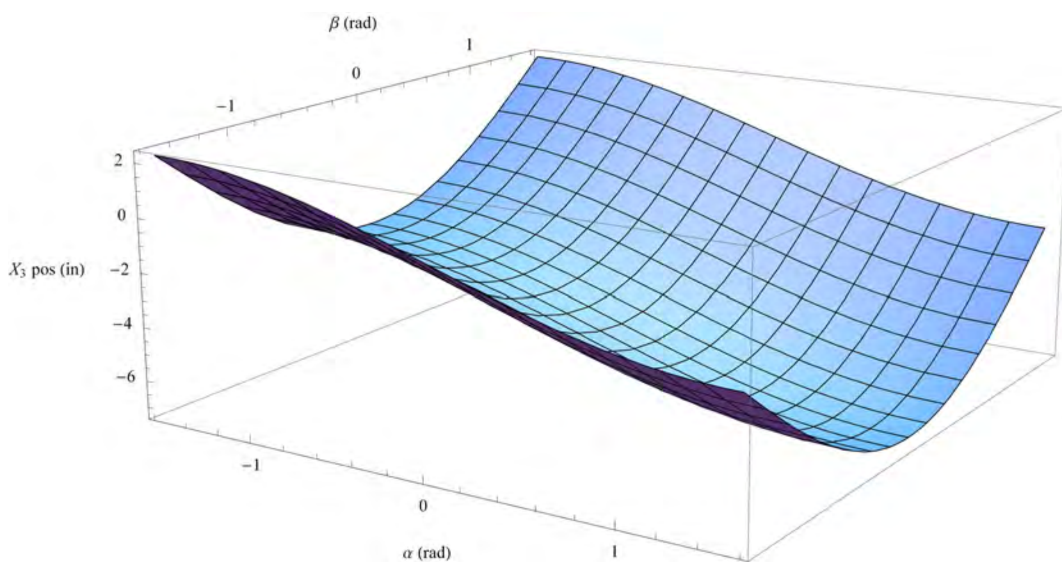

```
Plot3D[p[[3]] /. β → 0, {α, -π / 2, π / 2}, {γ, -π / 2, π / 2},
 AxesLabel → {"α (rad)", "β (rad)", "X3 pos (in)"}]
```

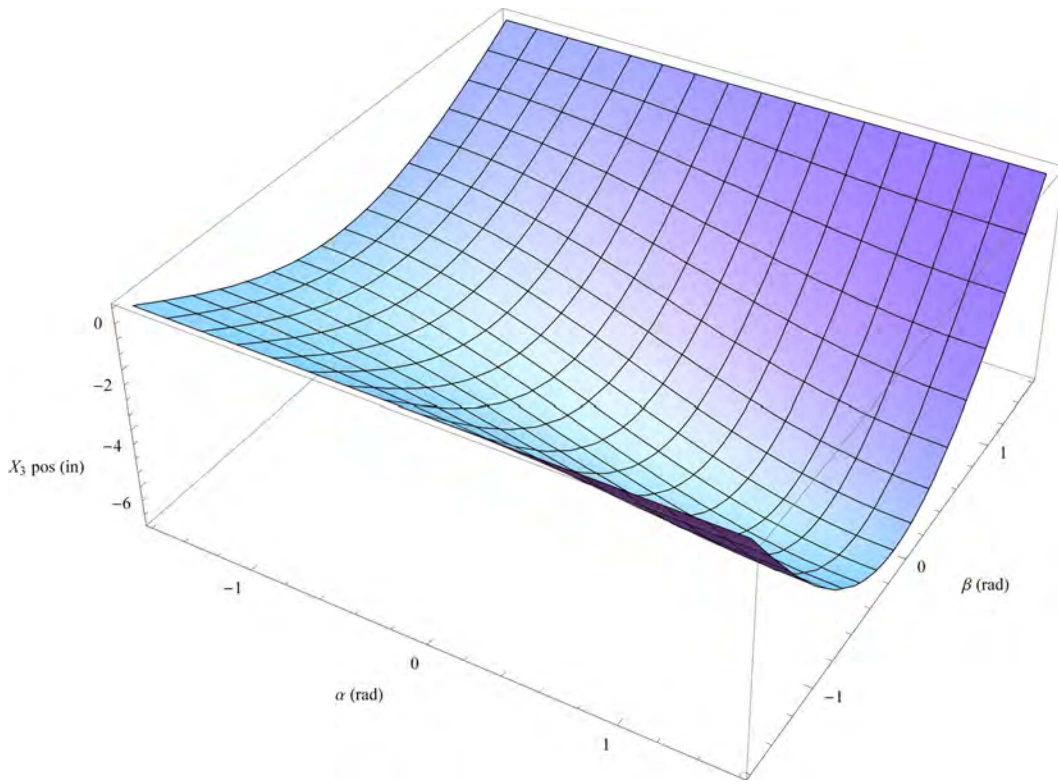


```
Plot3D[p[[3]] /. α → 0, {γ, -π / 2, π / 2}, {β, -π / 2, π / 2},
 AxesLabel → {"γ (rad)", "β (rad)", "X3 pos (in)"}]
```

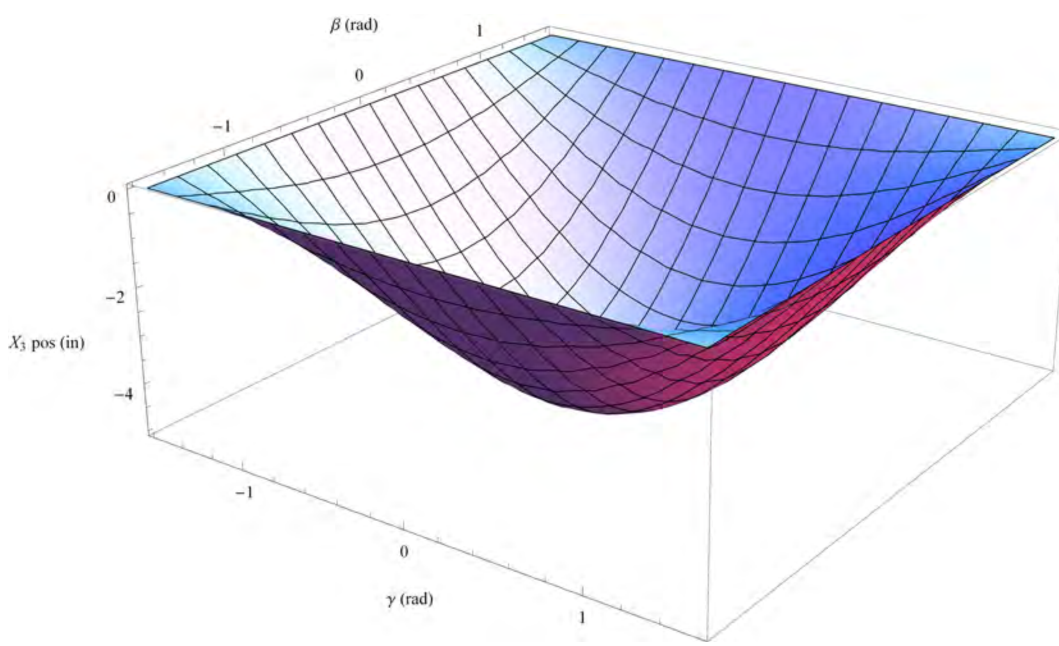

Closed Loops

There several loops of interest:
f to i to g to h to f
X to e to f to b to a to X
X to e to i2 to d to c to X

What are α and β in terms of θ_1, θ_2, and θ_3?

Method Used: Given two vectors in the same coordinate frame that follow different paths and end at the same point.
The difference of the two vectors, irrespective of the path, must equal zero.

```
γ → θ1(*Look at it... you'll see it*)
```

$\gamma \to \theta_1$

```
Linkage_cd = r_x2 + R2[θ2].(r_c + R1[ϕcd].r_d) /. Simple
Linkage_ed = r_x1 + R1[θ1].(r_e + R2[β].r_id) /. Simple
Loop1 = (Linkage_cd - Linkage_ed) / i_a == 0 // Simplify
```

$\{e_1 - \mathrm{Cos}[\phi_{cd}]\,\mathrm{Sin}[\theta_2]\,i_a,\ \mathrm{Sin}[\phi_{cd}]\,i_a,\ -\mathrm{Cos}[\theta_2]\,\mathrm{Cos}[\phi_{cd}]\,i_a\}$

$\{e_1 - \mathrm{Sin}[\beta]\,i_a,\ \mathrm{Cos}[\beta]\,\mathrm{Sin}[\theta_1]\,i_a,\ -\mathrm{Cos}[\beta]\,\mathrm{Cos}[\theta_1]\,i_a\}$

$\{\mathrm{Sin}[\beta] - \mathrm{Cos}[\phi_{cd}]\,\mathrm{Sin}[\theta_2],\ -\mathrm{Cos}[\beta]\,\mathrm{Sin}[\theta_1] + \mathrm{Sin}[\phi_{cd}],\ \mathrm{Cos}[\beta]\,\mathrm{Cos}[\theta_1] - \mathrm{Cos}[\theta_2]\,\mathrm{Cos}[\phi_{cd}]\} == 0$

```
Linkage_ab = r_x3 + R2[θ3].(r_a + R3[ϕab].r_b) /. Simple
Linkage_ef = r_x1 + R1[θ1].(r_e + R2[α].r_fb) /. Simple
Loop2 = (Linkage_ab - Linkage_ef) / b1 == 0 // Simplify
```

$\{\mathrm{Cos}[\theta_3]\,\mathrm{Cos}[\phi_{ab}]\,b_1 + e_1,\ \mathrm{Sin}[\phi_{ab}]\,b_1,\ -\mathrm{Cos}[\phi_{ab}]\,\mathrm{Sin}[\theta_3]\,b_1\}$

$\{\mathrm{Cos}[\alpha]\,b_1 + e_1,\ \mathrm{Sin}[\alpha]\,\mathrm{Sin}[\theta_1]\,b_1,\ -\mathrm{Cos}[\theta_1]\,\mathrm{Sin}[\alpha]\,b_1\}$

$\{-\mathrm{Cos}[\alpha] + \mathrm{Cos}[\theta_3]\,\mathrm{Cos}[\phi_{ab}],\ -\mathrm{Sin}[\alpha]\,\mathrm{Sin}[\theta_1] + \mathrm{Sin}[\phi_{ab}],\ \mathrm{Cos}[\theta_1]\,\mathrm{Sin}[\alpha] - \mathrm{Cos}[\phi_{ab}]\,\mathrm{Sin}[\theta_3]\} == 0$

```
eq1 = {Loop1[[1, 1]] / Sin[θ2] == 0, Loop1[[1, 3]] / Cos[θ2] == 0} // Simplify
eq2 = {Loop2[[1, 1]] / Cos[θ3] == 0, Loop2[[1, 3]] / Sin[θ3] == 0} // Simplify
```

$\{\mathrm{Cos}[\phi_{cd}] == \mathrm{Csc}[\theta_2]\,\mathrm{Sin}[\beta],\ \mathrm{Cos}[\phi_{cd}] == \mathrm{Cos}[\beta]\,\mathrm{Cos}[\theta_1]\,\mathrm{Sec}[\theta_2]\}$

$\{\mathrm{Cos}[\phi_{ab}] == \mathrm{Cos}[\alpha]\,\mathrm{Sec}[\theta_3],\ \mathrm{Cos}[\phi_{ab}] == \mathrm{Cos}[\theta_1]\,\mathrm{Csc}[\theta_3]\,\mathrm{Sin}[\alpha]\}$

```
eq1 = Tan[β] == Tan[β] eq1[[2, 2]] / eq1[[1, 2]]
eq2 = Tan[α] == Tan[α] eq2[[1, 2]] / eq2[[2, 2]]
```

$\mathrm{Tan}[\beta] == \mathrm{Cos}[\theta_1]\,\mathrm{Tan}[\theta_2]$

$\mathrm{Tan}[\alpha] == \mathrm{Sec}[\theta_1]\,\mathrm{Tan}[\theta_3]$

The following plots visualize the error when lettings $\alpha = \theta_3$ and $\beta = \theta_2$.

```
Plot3D[ArcTan[Sec[θ1] Tan[θ3]] - θ3, {θ1, -π / 2, π / 2},
 {θ3, -π / 2, π / 2}, AxesLabel → {"θ1 (rad)", "θ3 (rad)", "α - θ3 (rad)"}]
Plot3D[ArcTan[Cos[θ1] Tan[θ2]] - θ2, {θ1, -π / 2, π / 2}, {θ2, -π / 2, π / 2},
 AxesLabel → {"θ1 (rad)", "θ2 (rad)", "β - θ2 (rad)"}]
```

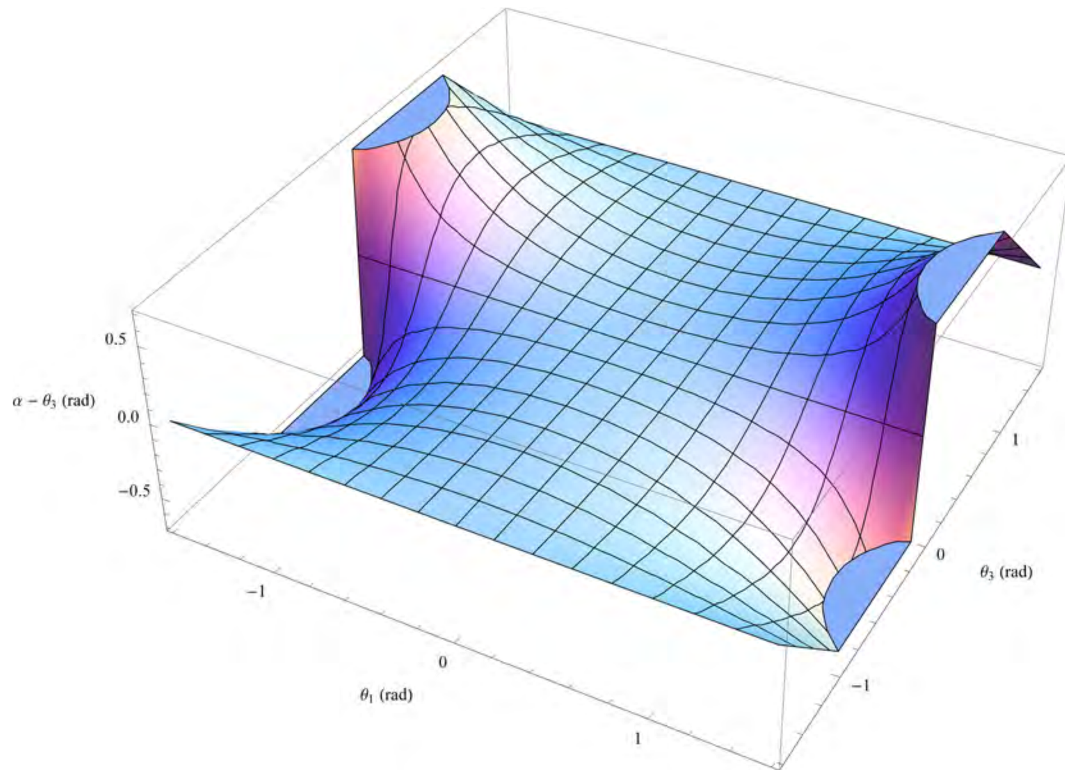

0.5
$\alpha - \theta_3$ (rad)
0.0
−0.5
−1
0
θ_1 (rad)
1
1
0
θ_3 (rad)
−1

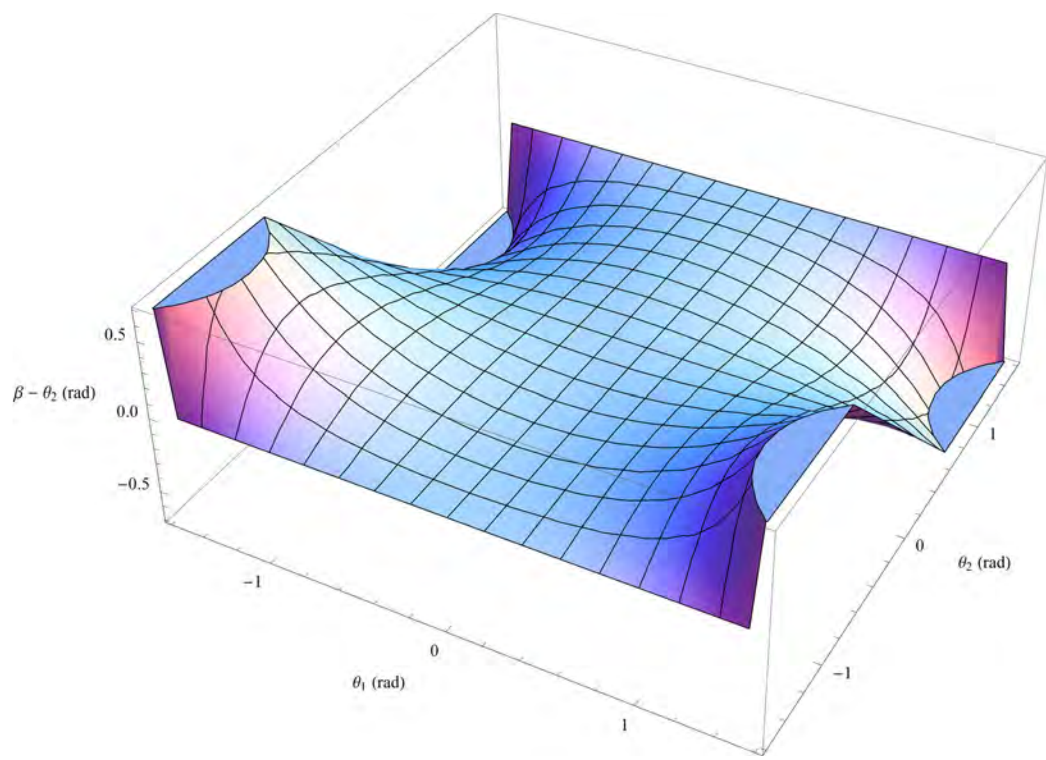

0.5
$\beta - \theta_2$ (rad)
0.0
−0.5
−1
0
θ_1 (rad)
1
1
0
θ_2 (rad)
−1

Appendix C

Code

C.1 Propeller Code

The following code was run on the propeller used to control the servos. The code allows the device to accept commands through the serial port which set the position of the servos. The code accepts the command 's#:val\r', where # is 1 through C, val is a numeric value, and \r is a carriage return. 'Servo32v7.spin' and 'Parallax Serial Terminal.spin' are available from the Parallax code exchange.

```
{{
****************************************
* Author: Daniel Trevitz          V1   *
* Purpose: Code is used to control 12   *
*    servos using a serial connection.  *
****************************************
}}

CON
    _clkmode = xtal1 + pll16x
    _xinfreq = 5_000_000      'Note Clock Speed for your setup!!

    _Servo_Center = 1500

    ServoCh1 = 0
    ServoCh2 = 1
    ServoCh3 = 2
    ServoCh4 = 3
    ServoCh5 = 4
    ServoCh6 = 5
    ServoCh7 = 6
    ServoCh8 = 7
    ServoCh9 = 24 'Mouse
    ServoChA = 25 'Mouse
    ServoChB = 26 'Keyboard
    ServoChC = 27 'Keyboard

OBJ
  SERVO : "Servo32v7.spin"
  DBG   : "Parallax Serial Terminal.spin"

PUB Servo_Control | cmd, moveVal

    DBG.Start(115200)
    SERVO.Start                 'Start Servo handler

    SERVO.Set(ServoCh1, _Servo_Center)
    SERVO.Set(ServoCh2, _Servo_Center)
```

```
    SERVO.Set(ServoCh3, _Servo_Center)
    SERVO.Set(ServoCh4, _Servo_Center)
    SERVO.Set(ServoCh5, _Servo_Center)
    SERVO.Set(ServoCh6, _Servo_Center)
    SERVO.Set(ServoCh7, _Servo_Center)
    SERVO.Set(ServoCh8, _Servo_Center)
    SERVO.Set(ServoCh9, _Servo_Center)
    SERVO.Set(ServoChA, _Servo_Center)
    SERVO.Set(ServoChB, _Servo_Center)
    SERVO.Set(ServoChC, _Servo_Center)

    repeat true

      DBG.StrIn(@cmd)         ' Get the command
      moveVal := DBG.DecIn  ' Get the value

      if(strcomp(@S1_Str, @cmd))
        SERVO.Set(ServoCh1, moveVal)
      elseif(strcomp(@S2_Str, @cmd))
        SERVO.Set(ServoCh2, moveVal)
      elseif(strcomp(@S3_Str, @cmd))
        SERVO.Set(ServoCh3, moveVal)
      elseif(strcomp(@S4_Str, @cmd))
        SERVO.Set(ServoCh4, moveVal)
      elseif(strcomp(@S5_Str, @cmd))
        SERVO.Set(ServoCh5, moveVal)
      elseif(strcomp(@S6_Str, @cmd))
        SERVO.Set(ServoCh6, moveVal)
      elseif(strcomp(@S7_Str, @cmd))
        SERVO.Set(ServoCh7, moveVal)
      elseif(strcomp(@S8_Str, @cmd))
        SERVO.Set(ServoCh8, moveVal)
      elseif(strcomp(@S9_Str, @cmd))
        SERVO.Set(ServoCh9, moveVal)
      elseif(strcomp(@SA_Str, @cmd))
        SERVO.Set(ServoChA, moveVal)
      elseif(strcomp(@SB_Str, @cmd))
        SERVO.Set(ServoChB, moveVal)
      elseif(strcomp(@SC_Str, @cmd))
        SERVO.Set(ServoChC, moveVal)



DAT
  S1_Str byte "s1:",0
  S2_Str byte "s2:",0
  S3_Str byte "s3:",0

  S4_Str byte "s4:",0
  S5_Str byte "s5:",0
  S6_Str byte "s6:",0

  S7_Str byte "s7:",0
  S8_Str byte "s8:",0
  S9_Str byte "s9:",0

  SA_Str byte "sA:",0
  SB_Str byte "sB:",0
  SC_Str byte "sC:",0
```

C.2 Motion Sequences

All of these motions are designed to be repeating. That is to say the start point and end point are the same. 'move()' is a function the commands each servo in the robot. The robot is split into quadrents, looking from the top down. The function is then defined as move(S1_Q1, S2_Q1, S3_Q1, S1_Q2, S2_Q2, S3_Q2, S1_Q3, S2_Q3, S3_Q3, S1_Q4, S2_Q4, S3_Q4). zero() moves all servos to the standard anatomical position.

C.2.1 Sit

```
zero();
usleep(500000);
move(0,-30,-70,  0,-30,-70,   0,60,26,  0,60,20);
sleep(3);
zero();
```

C.2.2 Lay

```
zero();
move(0,90,60,0,90,60,0,-90,-60,0,-90,-60);
move(0,0,30,0,0,30,0,-90,-60,0,-90,-60);
move(0,0,30,0,0,30,0,0,30,0,0,30);
zero();
```

C.2.3 Kicking a Ball

```
zero();
move(0,-2,-40,0,  8, 21,0,4,-20,0,5,26);
move(0,-2,-40,0,-40,-40,0,4,-20,0,5,26);
usleep(500000);
move(0,-2,-40,0, 40,  0,0,4,-20,0,5,26);
zero();
```

C.2.4 Stair Climbing

```
zero();

///Foot one up
"move(0,-2,35,0,8,-50,0,4,26,0,5,-30);"

//Foot one on step 1
"move(0,30,18,0,8,-50,0,4,26,0,5,-30);"

//Foot two up
"move(0,30,18,-52,8,25,0,4,23,0,5,20);"
"move(0,30,18,-52,65,25,0,4,23,0,5,20);"
"move(0,30,18,0,65,25,0,4,23,0,5,20);"
"move(0,30,18,0,41,30,0,4,23,0,5,20);"

//Forward
move(0,0,-3,0,0,15,0,-30,-10,0,-30,-10);

"move(0,0,-31,0,0,15,0,-30,-47,0,-30,13);"
"move(0,0,-31,0,0,15,0,-30,-47,0,34,22);"
"move(0,0,2,0,0,15,0,-30,-47,0,34,-14);"
"move(0,-20,2,0,-20,15,0,-30,-2,0,0,20);"

//Foot one and two on step 2
"move(0,-20,2,0,-20,-68,0,-20,13,0,0,-42);"
"move(40,-20,17,0,-20,-68,0,-20,13,0,0,-42);"
"move(40,20,17,0,-20,-68,0,-20,13,0,0,-42);"
"move(0,20,17,0,-20,-68,0,-20,13,0,0,-42);"
"move(0,20,1,0,-20,-68,0,-20,13,0,0,-42);"
"move(0,20,1,0,-20,-68,0,-20,13,0,0,12);"
"move(0,20,1,0,-20,17,0,-20,11,0,0,12);"
"move(0,20,1,-54,-20,17,0,-20,11,0,0,12);"
"move(0,20,1,-54,36,17,0,-20,11,0,0,12);"
"move(0,20,-43,-24,36,17,0,-20,11,0,0,12);"
"move(0,8,-47,4,24,17,0,-20,-14,0,0,12);"
"move(0,8,-47,0,17,3,0,-20,-14,0,0,12);"

//Shift weight
move(0,-20,-47,0,0,3,0,-40,-14,0,-20,12);

//Put foot one up
"move(0,-20,-47,0,0,3,0,-40,-14,0,-20,12);"
"move(0,-20,-14,10,0,-40,0,-40,-14,0,-20,-50);"
"move(0,31,20,10,0,-40,0,-40,-14,0,-20,-50);"

//Lunge
"move(0,31,-6,10,-20,-40,0,-50,-14,0,-40,-50);"


//Leg 2 up
"move(0,31,-10,10,-20,-40,0,20,-20,0,-40,-50);"
```

```
"move(0,31,-10,10,-20,-40,0,10,-15,0,-40,4);"
"move(0,31,-10,10,-52,-1,0,10,-15,0,-40,4);"
"move(0,31,-10,-74,-52,-1,0,10,-15,0,-40,4);"
"move(0,31,-10,-74,33,-1,0,10,-15,0,-40,4);"
"move(0,31,-10,-52,46,-1,0,10,-15,0,-40,4);"
"move(0,31,-10,-37,61,-1,0,10,-15,0,-40,4);"
"move(0,31,-10,0,61,-1,0,10,-15,0,-40,4);"
"move(0,31,-10,0,47,-1,0,10,-15,0,-40,4);"
```

Appendix D

Tools and Materials

D.1 Materials

Very few materials were used for the prototypes. The first prototypes where made from Legos, with the remaining made from varying quantities of the following parts list:

1. Colored Cast Acrylic Sheet .236" Thick, 36" X 48"
   McMaster-Carr # 505K962
2. Acrylic Sheet 1/4" Thick, 12" X 12"
   McMaster-Carr # 8589K81
3. 18-8 Stainless Steel, 5-40 Thread, 3' Threaded rod
   McMaster-Carr # 98847A006
4. 18-8 Stainless Steel, 100 Undersized Hex Nut, 5-40 Thread Size, 1/4" Width, 3/32" Height
   McMaster-Carr # 90730A006
5. 18-8 Stainless Steel, 100 Flat Washer, No. 5 Screw Size, 9/32" OD, .02"-.04" Thick
   McMaster-Carr # 92141A006
6. 18-8 Stainless Steel, 100 Pan Head Screw, 4-40 Thread, 1/4" Length
   McMaster-Carr # 91772A106

D.2 Software Tools

A few software packages were used throughout the course of the thesis. The primary application was 2012 SolidWorks, provided by the university. All of the parts were solid modeled in SolidWorks first. After solid modeling, the parts were merged with the correct quantity of each part for the current prototype, onto a single two dimensional drawing. The drawing was converted to DXF format by SolidWorks and then cleaned and verified, for use with the laser cutter, with either DeltaCAD, LibreCAD, or Corel Draw.

The thesis used a Parallax Propeller microcontroller to control the servos. The microcontroller was programed using the proprietary Propeller Tool IDE. An existing servo controller class was added to some custom code to make the microcontroller into a twelve servo controller. The servos could be repositioned with a serial port command.

The microcontroller was controlled by a custom program. The program was developed in the Qt Creator IDE using the Qt4 library suit for the Linux OS. The custom program allowed the code from Section-C.2 to be evaluated as a scripted language.

D.3 Mechanical Tools

Several tools were selected for machining the parts. The machining was first done with an Epilog Helix 24, 60 Watt, CO_2 Laser cutter. The Helix 24 can cut a sheet of 18" x 24" x 0.25" acrylic. The robot presented in this thesis required a single sheet of this size.

Figure D.1: Epilog Helix 24 Stock Photo from `http://www.epiloglaser.com/`

After the parts were cut by the laser cutter, they were machined with a drill press. The drill press used, shown in Figure-D.2, is a precision press allowing for the accuracy needed. The majority of the parts needed the #38 drill bit to pre-drill the hole for the 5-40 tap. The 5-40 tap was used to thread the plastic for the threaded rod. The #43 bit was used to make the holes for the 4-40 tap and to make some pilot holes. The 4-40 tap threaded the holes for the 1/4" 4-40 screws. The 1/8" bit was used for the remaining holes to allow for rotation of the 5-40 threaded rod within the hole.

Figure D.2: Family owned, Sensitive Drilling Machine

The following items, shown in Figure-D.3, are a list of tools purchased for this thesis:

1. Tap Wrench, T-Handle Style, 0 - 1/4" Tap Size
   McMaster-Carr # 25605A63

2. Carbon Steel Hand Bottoming Tap, 4-40, 3 Flute
   McMaster-Carr # 25995A165

3. General Purpose High-Speed Steel Hand Bottoming Tap, 5-40, H2 Pitch Diameter, 3 Flute
   McMaster-Carr # 2522A736

4. General Purpose High-Speed Steel Hand Plug Tap, 5-40, H2 Pitch Diameter, 3 Flute
   McMaster-Carr # 2522A716

5. General Purpose Drill Bit, Wire Gauge 43
   McMaster-Carr # 2901A217

6. General Purpose Drill Bit, Wire Gauge 38
   McMaster-Carr # 2901A212

7. General Purpose Drill Bit, 1/8"
   McMaster-Carr # 2901A115

The remaining tools were found to be needed to construct the prototypes. Take note that the red wire strippers in Figure-D.3 were filed to allow the flat surface to tighten nuts at the low clearance areas.

Figure D.3: Hand tools used in the thesis

The following is a list of notes for future work:

- The 4-40 tap was a far lower quality tap and the edge was lost in under 2 months due to corrosion.
- The plug tap, while leaving the bottom of the hole untapped, was much easier to reliably start in the plastic. It is possible to use the plug tap for part of the hole, then switch to the bottoming tap if a fully threaded hole is needed.
- The 1/4" screws where, in general, 1/8" too short to fully secure any part, and often pulled out of the plastic.
- Any time the 1/8" bit was used a smaller pilot hole had to be drilled to prevent the bit from grabbing and braking the part. The problem was alleviated, but not eliminated, by filing down the edge of the 1/8" bit.
- The difference between the 4-40 and 5-40 thread size is minimal. A 5-40 screw could be used instead of the 4-40 screw, at the cost of slightly increased hole size. While prototyping, the act of switching between bits and taps was found to be tedious.
- An attempt of using a Dremel to cut the threaded rod was made. The Dremel was found to be far more trouble then using a simple, sharp, hack saw.
- When cutting the threaded rod, it is necessary to remove any burrs from the threads to ensure the plastic threads will not be gouged.

Bibliography

[1] Chernyak, V., T. Flynn, J. O'Rourke, J. Morgan, A. Zalutsky, S. Chernova, S. Nestinger, and T. Padir (2012) "The Design and Realization of a High Mobility Biomimetic Quadrupedal Robot," in *Mechatronics and Embedded Systems and Applications (MESA), 2012 IEEE/ASME International Conference on*, vol. 58, pp. 93–98.

[2] Adelstein, B. D. (1998), "Three Degree of Freedom Parallel Mechanical Linkage," .

[3] Miller, P. (2004) *Mechanical Design, Modeling, and Control of a Three Degree-of-Freedom Parallel Mechanism with Two-Dimensional Inverted Pendulum*, Master's thesis, University of Illinois.

[4] Adelstein, B., P. Ho, and H. Kazerooni (1996) "Kinematic Design of a Three Degree of Freedom Parallel Hand Controller Mechanism," **58**, pp. 539–546.

[5] Hurbain, P. (2012), "LEGO® 9V Technic Motors compared characteristics," .
URL `http://www.philohome.com/motors/motorcomp.htm`

[6] de Santos, P., E. García, and J. Estremera (2012) *Quadrupedal Locomotion: An Introduction to the Control of Four-legged Robots*, Springer.

[7] Manseur, R. (2007) *Robot modeling and kinematics*, Firewall Media.

[8] Carl D. Crane, I. and J. Duffy (2008) *Kinematic Analysis of Robot Manipulators*, Cambridge University Press.